MAUSAM, 51, 2 (April 2000) 127-154

551.553.21 : 551.585.3(94)

The Australian monsoon Part-I : Climatological features and the Asian connection

KSHUDIRAM SAHA

27, B-Road, Maharani Bagh, New Delhi-110 065, India

and

SURANJANA SAHA

Environmental Modelling Center, NCEP/NOAA
Washington, D.C., U.S.A.
(Received 8 April 1999)

सार - एन.सी.ई.पी./एन.सी.ए.आर. के द्वारा किए गए पुनः विश्लेषणों से ज्ञात हुई ऑस्ट्रेलिया के ग्रीष्मकालीन मानसून से संबद्ध अनेक मौसम वैज्ञानिक विभिन्नताओं के जलवायविक क्षेत्रों की समीक्षा, इस महाद्वीप तथा इसके आसपास के क्षेत्रों में पाए गए मौसम और जलवायु के परिप्रेक्ष्य में की गई है। दाब, तापमान एवं परिसंचरण की विशेषताओं के अन्तरगोलार्द्ध वितरणों से यह पता चलता है कि ग्रीष्म एवं शीत दोनो ऋतुओं के दौरान ऑस्ट्रेलिया और एशिया के मानसून के संबंधों में उतार-चढाव पाया गया है। भूमध्यरेखा के उस पार के वायु के फ्लक्सों के परिकलित मान इस अनुमान की पुष्टि करते हैं।

ABSTRACT. Climatological fields of several meteorological variables associated with the Australian summer monsoon, as revealed by NCEP/NCAR reanalysis, are reviewed in the context of observed weather and climate over the continent and surrounding regions. Inter-hemispheric distributions of pressure, temperature and circulation features suggest a see-saw relationship of the Australian monsoon with the monsoons of Asia during both summer and winter. Computed values of cross-equatorial fluxes of air appear to lend credence to this hypothesis.

Key words – Australian monsoon, Climatology of Australia, Inter-hemispheric transport of air, Cross-equatorial fluxes.

1. Introduction

The continent of Australia, situated between latitudes about 10°S and 43°S and longitudes about 113°E and 153°E, experiences its summer monsoon during the months of December to February. The equatorial trough (ET) of low pressure and its associated inter-tropical convergence zone (ITCZ) is then located a few degrees south of the equator, usually between about 5°S and 15°S, over most parts of the equatorial/tropical Indian Ocean and the Western Pacific. At the ET, the low-level trades of the two hemispheres, *viz.*, the southeast trades of the southern hemisphere and the northeast trades of the northern hemisphere, which after crossing the equator turn into west-northwesterlies, meet producing a narrow zone of low-level convergence and precipitation. However, over Australia, the ET is drawn much further south by a 'heat low' that develops over the continent due to land-sea thermal contrast and is centred at surface near 25°S, mainly over the western part of the continent. The 'heat low', which may be looked upon as a perturbation in the subtropical high-pressure belt of the southern hemisphere, maintains its own circulation, though interacting with the trade-winds of the two hemispheres. Quite often, the 'heat low' circulation interacts with lows, depressions and cyclones that form over the tropical part of Australia and adjoining sea areas in the north and mid-latitude baroclinic disturbances that move across the southern part of the continent. Thus, a knowledge and understanding of these interactions would seem to constitute a pre-requisite to a fuller understanding of the continent's weather and climate.

Early studies of the Australian summer monsoon, such as those by Troup (1961), Berson and Troup (1961) and Gentilli (1971), were done with rather limited surface

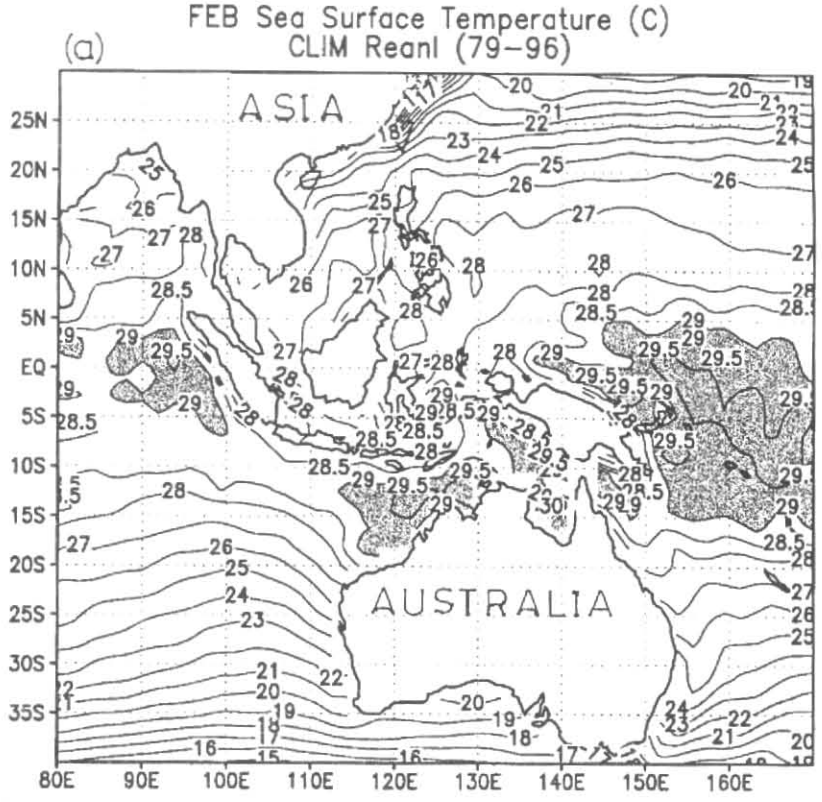

Fig. 1(a). Distribution of reanalysis 18-year (1979-96) mean sea surface temperature (SST) over the Indian and Pacific oceans surrounding Australia during February (unit : C)

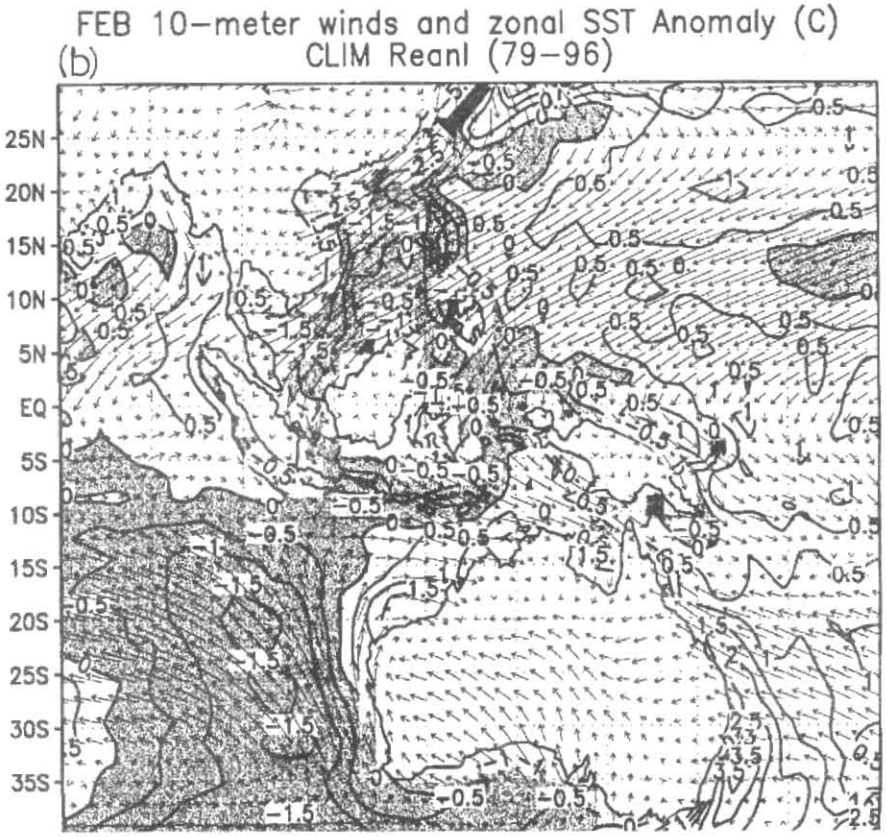

Fig. 1 (b). Same as (a), but for the zonal anomaly (deviation from the zonal mean) of SST and 10m-winds

and aero-logical data. However, following improvement in data situation during the FGGE Northern Hemisphere Winter Monsoon Experiment (WMONEX), 1978-79, there was a spurt in research activity and several studies (*e.g.*, Sumi and Murakami, 1981; Murakami and Sumi, 1982 a,; Nicholls *et al.*, 1982, 1984 a,b; Davidson *et al.*, 1983 and 1984; McBride, 1983; McBride and Nicholls, 1983; Love and Garden, 1984; Pittock, 1984; Love, 1985 a,b; Holland and Nicholls, 1985) were undertaken on such diverse aspects of the Australian monsoon as its onset and structure, divergent circulations, active and break monsoons, intra-seasonal oscillations, tropical-mid-latitude interactions, monsoon depressions and cyclones, influence of El-Nino Southern Oscillations (ENSO) on Australian rainfall and other related weather phenomena. Quite a few of these studies (*e.g.,* Davidson *et al.*, 1983) referred to the Australian summer monsoon as being similar to the Asian/Indian summer monsoon in the northern hemisphere. Holland (1984 a,b,c) made a special study of the climatology and structure of tropical cyclones in the Australian/Southwest Pacific region. These and several other studies contributed significantly to our knowledge and understanding of the Australian summer monsoon. An excellent review of some of these studies by McBride appears in Chang and Krishnamurti (1987).

However, notwithstanding significant progress made, gaps and uncertainties remain in several areas. For example, the effect of interaction of the 'heat low' circulation with the tradewinds of the two hemispheres on the continent's weather and climate needs to be investigated in greater detail. Practically the whole of Western and South-Central Australia is a vast desert. As against this, a lot of rain falls over northern Australia and the windward slopes of the Great Dividing Range and the Australian Alps which run almost north-south along the eastern seaboard of the continent. The cause of this great disparity in the distribution of rainfall needs to be investigated further. The role of the West Australian cold ocean current in the making of the continent's weather and climate especially its possible influence, along with several other factors, on the formation of monsoon disturbances need to be looked into more closely. Several hypotheses have been advanced regarding the formation, development and movement of depressions and cyclones in the Australian region but the key question as to what triggers these disturbances still remains to be resolved (*e.g.,* Davidson *et al.*, 1983). Also, in the circulation field, the exact manner in which the monsoon cell co-exists with the Hadley cells of the two hemispheres remains to be demonstrated. A possible connection of the Australian monsoon to its counterpart over Asia which has been mentioned in literature needs to be investigated further. Cross-equatorial fluxes and inter-hemispheric movement of air in the Australian region in both the lower and the upper troposphere during austral summer and winter have been noted in the past (*e.g.,* Sumi and Murakami, 1981; Davidson *et al.*, 1983; Tao and Chen, 1987) but a quantitative measure of these fluxes is still not available. It is proposed to address some of these problems in the present study, using recent global data analysis for the month of February when the Australian summer monsoon is fully developed. To bring out the seasonal contrast, some aspects of the Australian winter monsoon will also be projected.

Results of the study are presented in two parts. Part 1 deals with the structure of the general climatological fields of several meteorological variables, such as sea surface temperature (SST), atmospheric temperature and pressure, wind, humidity, precipitation, etc., and also such derived parameters as divergence, vorticity, vertical motion, diabatic heating, etc., and seeks to relate these fields with circulation features and observed weather and climate. Part 2 addresses the problem of cyclogenesis that leads to development of depressions and cyclones in the Australian region.

2. Analysis

Global data analysis utilized in the present study is that recently prepared by the National Centres for Environmental Prediction (NCEP)\National Centre for Atmospheric Research (NCAR) under a special project called reanalysis (Kalnay *et al.*,1996). As designed, the project aims to produce a 40-year record of global analysis of atmospheric fields for use of climate researchers. As stated by Kalnay *et al.,* (1996), it uses a frozen state-of-the-art global data assimilation system (GDAS) and a database as complete as possible. The data assimilation system and the model used are identical to the global system implemented operationally at the NCEP on 11 January 1995, except that the hortizontal resolution is T62 (about 210 km). The database has been enhanced with many sources of observations not available in real time for operations, provided by different countries and organizations. The system has been designed with advanced quality control and monitoring components and can produce one month of reanalysis in one day on a Cray YMP/8 supercomputer.

For study of the climatological of the Australian summer monsoon, the authors used an 18-year (1979-96) mean reanalysis for February of selected climatic variables at surface and isobaric surfaces 925, 850, 700, 500, 300, 200 and 100 hPa over an area bounded by the latitudes 40°S and 30°N and the longitudes 80°E and 170°E. Surface variables include SST, mean sea level pressure and rainfall, while upper-air variables are the virtual temperature, wind, geo-potential heights, specific

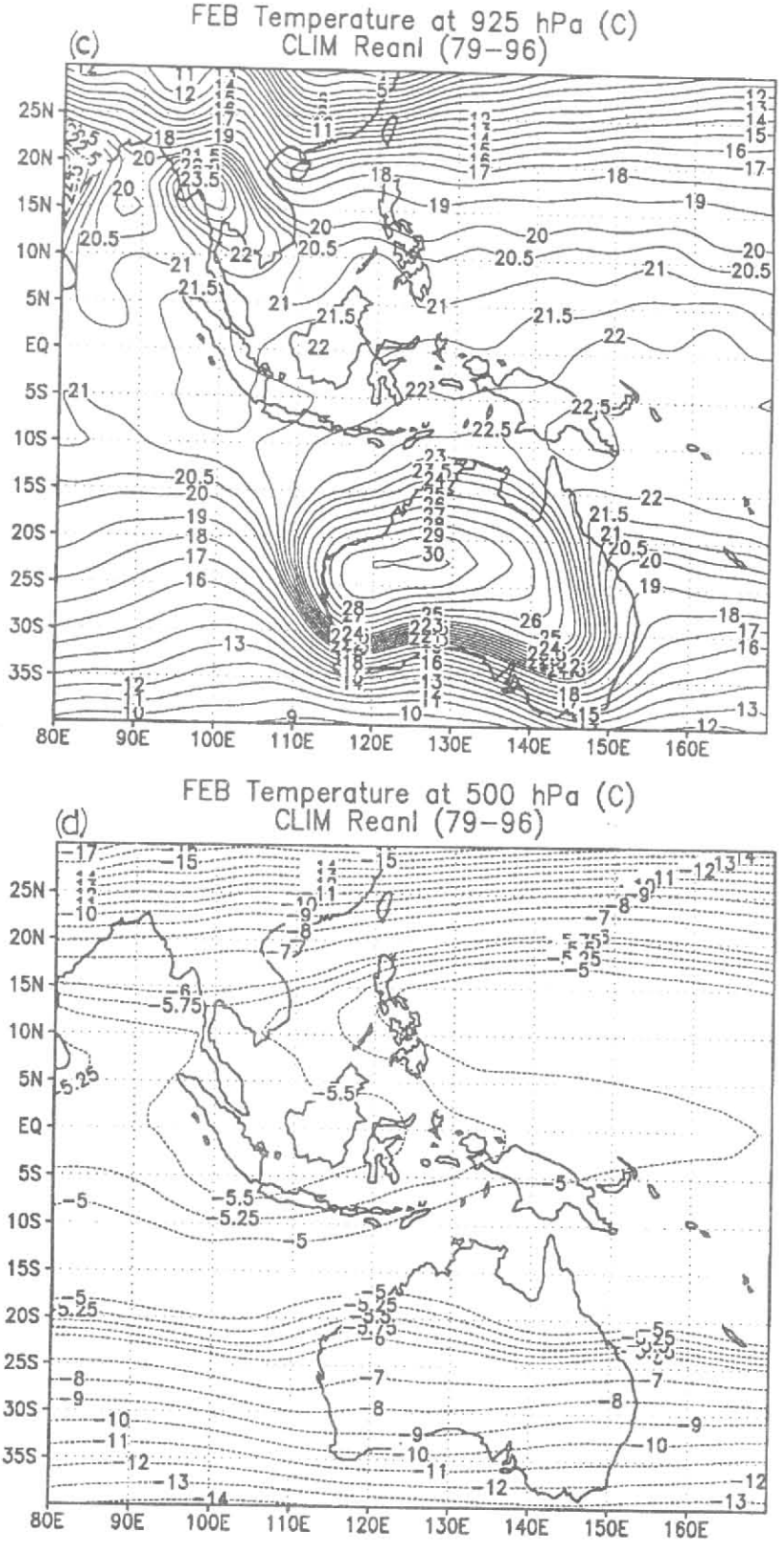

Figs.1 (c&d). Temperature fields (C) at 925 and 500 hPa over Australia and surrounding areas

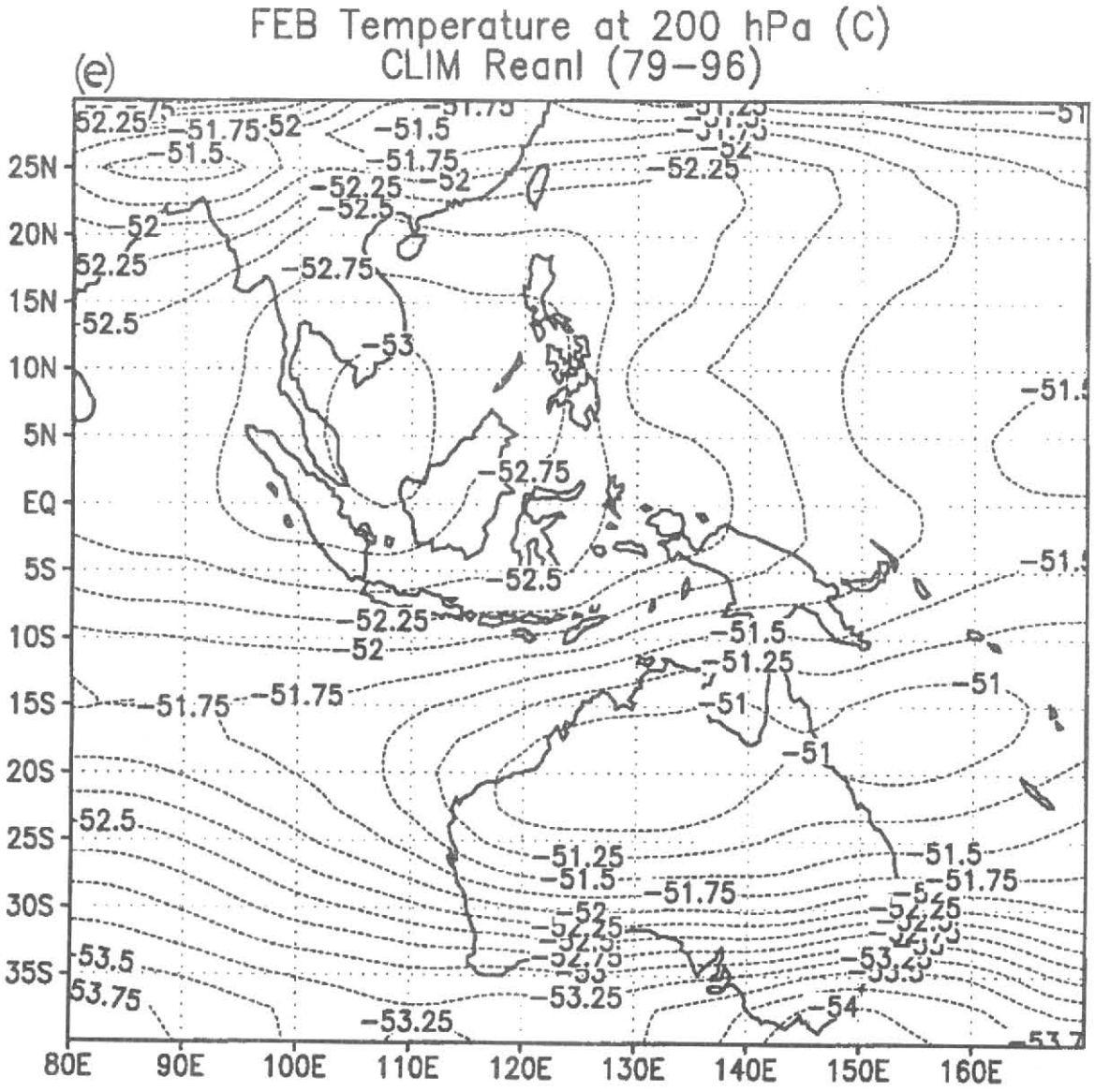

Fig.1 (e). Temperature fields (C) at 200 hPa over Australia and surrounding areas

humidity, divergence, vorticity, vertical velocity, and diabatic heating at the standard pressure surfaces. The reanalysis scheme makes a distinction between the different types of analysis obtained depending on the degree to which the analysis is influenced by the observations and or the model. Amongst the variables the analyses of which are influenced to the maximum by the observations are the SST and the upper-level wind, temperature and isobaric heights. Specific humidity and vertical velocity are amongst those variables the analysis of which are influenced by both observations and the model. The analyses of precipitation, diabatic heating and OLR are totally model-dependent and, therefore, less reliable than the basic parameters from which they are derived.

3. Structure of basic climatological fields

Structure of some of the basic climatological fields, such as temperature, pressure, isobaric heights, wind, humidity and precipitation is studied in this section. However, for lack of space, a restriction had to be placed on the number of upper-air surfaces at which the analyses could be presented. Therefore, three surfaces, *viz.*, 925,

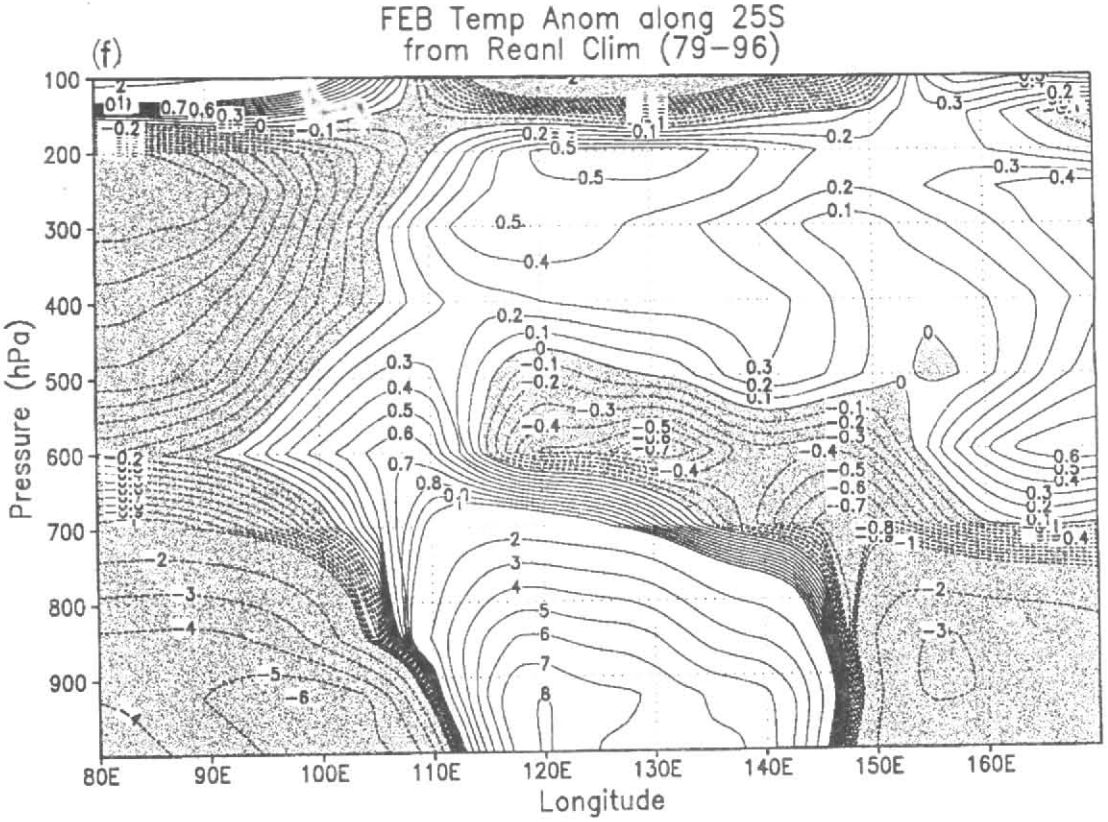

Fig. 1 (f). Vertical distribution of zonal anomaly of temperature (C) along 25°S

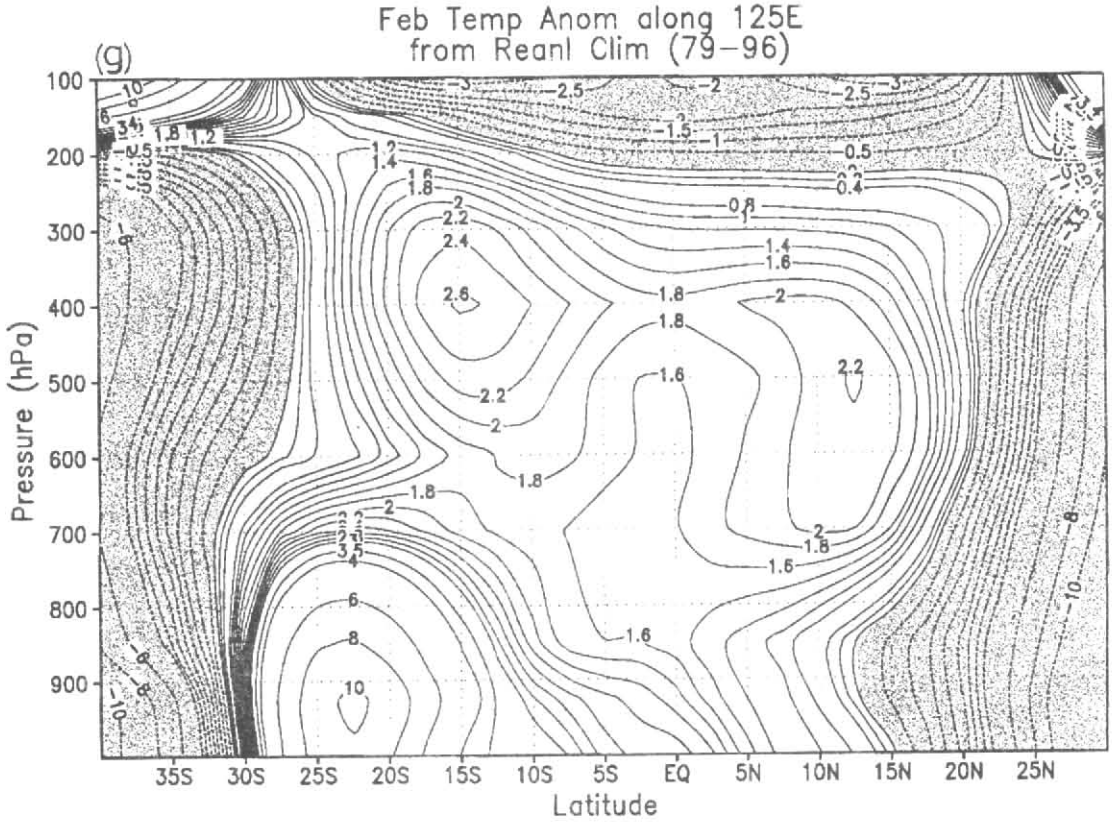

Fig. 1 (g). Vertical distribution of meridional anomaly (deviation from the meridional mean) of temperature (C) along 125°E

500 and 200 hPa were chosen to represent conditions in the lower, middle and upper troposphere respectively. The findings in respect of the different variables may be briefly summarised as follows :

3.1. *Temperature*

3.1.1. *Sea surface temperature (SST)*

Since Australia is surrounded by oceans, a study of the sea surface temperature around the continent assumes great importance. In Fig. 1 are presented: (a) the distribution of mean February SST over the Indian and Pacific oceans and (b) February SST zonal anomaly together with the winds at the 10 m height, as obtained from the reanalysis. Together, Figs. 1(a & b) would appear to show the following :

(*i*) Over the Indian Ocean, westward of the coast of southwestern Australia, say along 25°S, there is a strong cold anomaly up to about 80°E and then a warm anomaly which extends as far west as the east coast of South Africa.

(*ii*) The area of cold anomaly off the coast of Western Australia appears to extend north-westward also towards the equatorial western Indian Ocean.

(*iii*) The sea surfaces to the northwest of north-western Australia appears to be appreciably warm, as also the entire equatorial eastern Indian Ocean which lies to its northwest.

(*iv*) SST appears to decrease almost uniformly across the equator from the coast of northern Australia towards the Asian continent.

(*v*) The equatorial Pacific Ocean, east of longitude about 150°E, appears to be very warm with the highest mean SST of about 29.5°C located between about 5°N and 15°S.

(*vi*) In sharp contrast with the coldest anomaly over the Indian Ocean off the coast of south-western Australia, a strong warm anomaly appears over the Pacific just east of the coast of South-eastern Australia.

(*vii*) The 10 m-wind field shows the strong trade-winds at the two hemispheres, their meeting along the ET/ITCZ a few degrees south of the equator and the unusually strong southerlies over the Indian Ocean just off the coast of south-western Australia.

3.1.2. *Tropospheric temperature fields*

The time-mean February temperature fields at 925, 500 and 200 hPa are presented in Figs. 1 (c-e) respectively.

At 925 hPa [Fig. 1(c)], a pressure surface lying close to the mean topographic height of Australia, the highest mean temperature of about 30°C is located over the western part of the continent and the temperatures over the land surface are generally higher than those over the oceans all round. The land-sea thermal contrast stands out in both the zonal and meridional directions. The distribution of temperature at 925 hPa shows that while there is little or no temperature gradient across the equator in the Bay of Bengal sector and in the western Pacific (east of New Guinea), temperature decreases almost uniformly from Australia to Asia across the Maritime continent.

At 500 hPa [Fig. 1(d)] , the warmest temperature over the Indian Ocean appears south of the equator between about 10°S and 20°S, while, two warm belts appear over the Australian longitudes, one south of the equator between about 5°S and 20°S and the other north of the equator between about 5°N and 15°N. The equatorial region over the Australian longitudes appears to be cold.

At 200 hPa [Fig. 1(e)] a warm belt with the maximum temperature exceeding -51°C is located over Australia between longitudes about 15°S and 25°S. Over the Indian Ocean region, two warm belts may be seen, one south of the equator between about 10°S and 20°S and the other north of the equator over the Asian continent, with cold temperatures in between over the equatorial belt.

3.1.3. *Vertical cross-sections of temperature*

Two vertical sections through the temperature anomaly field over Australia are presented, one zonal along 25°S in Fig. 1(f) and the other meridional along 125°E in Fig.1(g).

Fig. 1(f) which presents the zonal anomaly (deviation from the zonal mean) of temperature along latitude 25°S, shows that in the lower troposphere below about 500 hPa, a strong warm anomaly lies over the Australian continent, flanked by two cold anomalies, one located over the Pacific Ocean to the east and the other over the Indian Ocean to the west. The axes of both the warmest and the coldest anomalies appear to tilt westward with height. Above about 500 hPa, the warmest (coldest) anomaly appears to be located almost vertically above the lower-tropospheric warmest (coldest) anomaly.

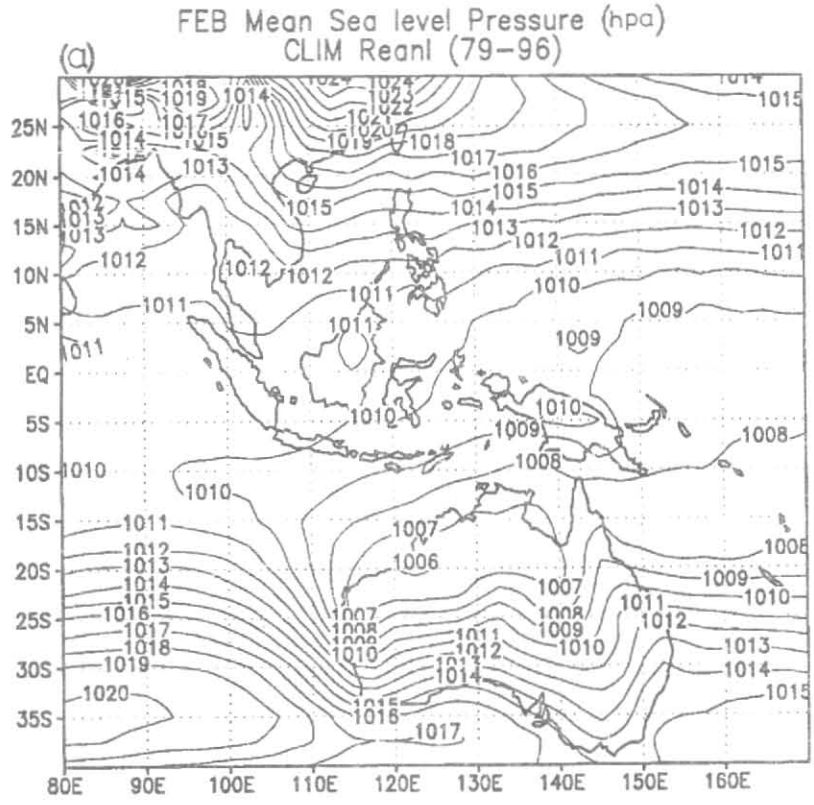

Fig. 2 (a). February Mean sea level pressure (hPa)

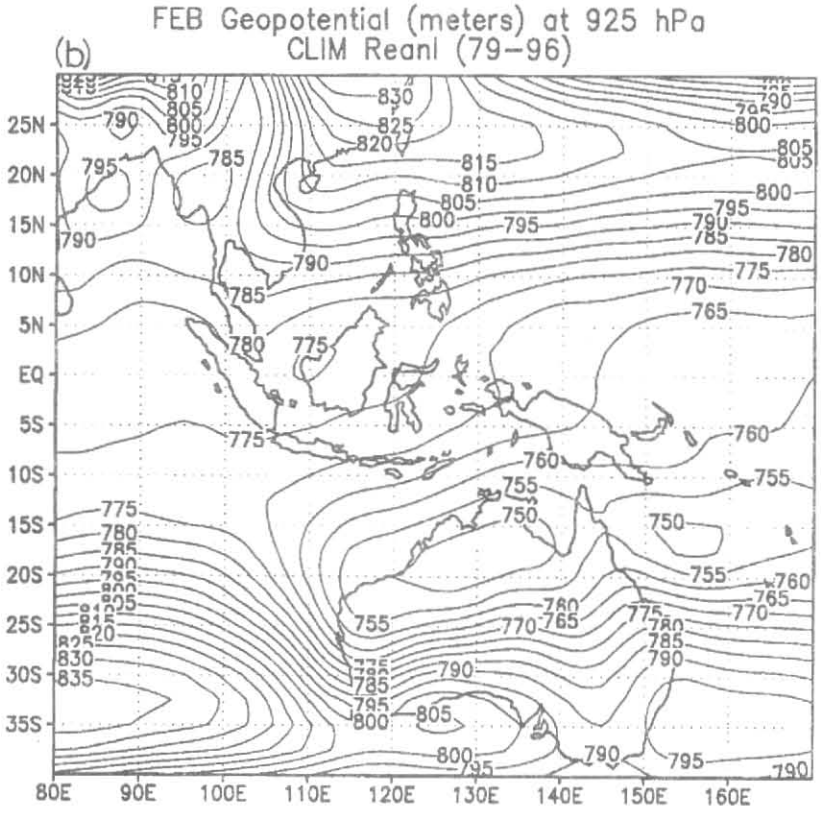

Fig. 2 (b). Geopotential height (gpm) fields at 925 hPa over Australia and surrounding areas

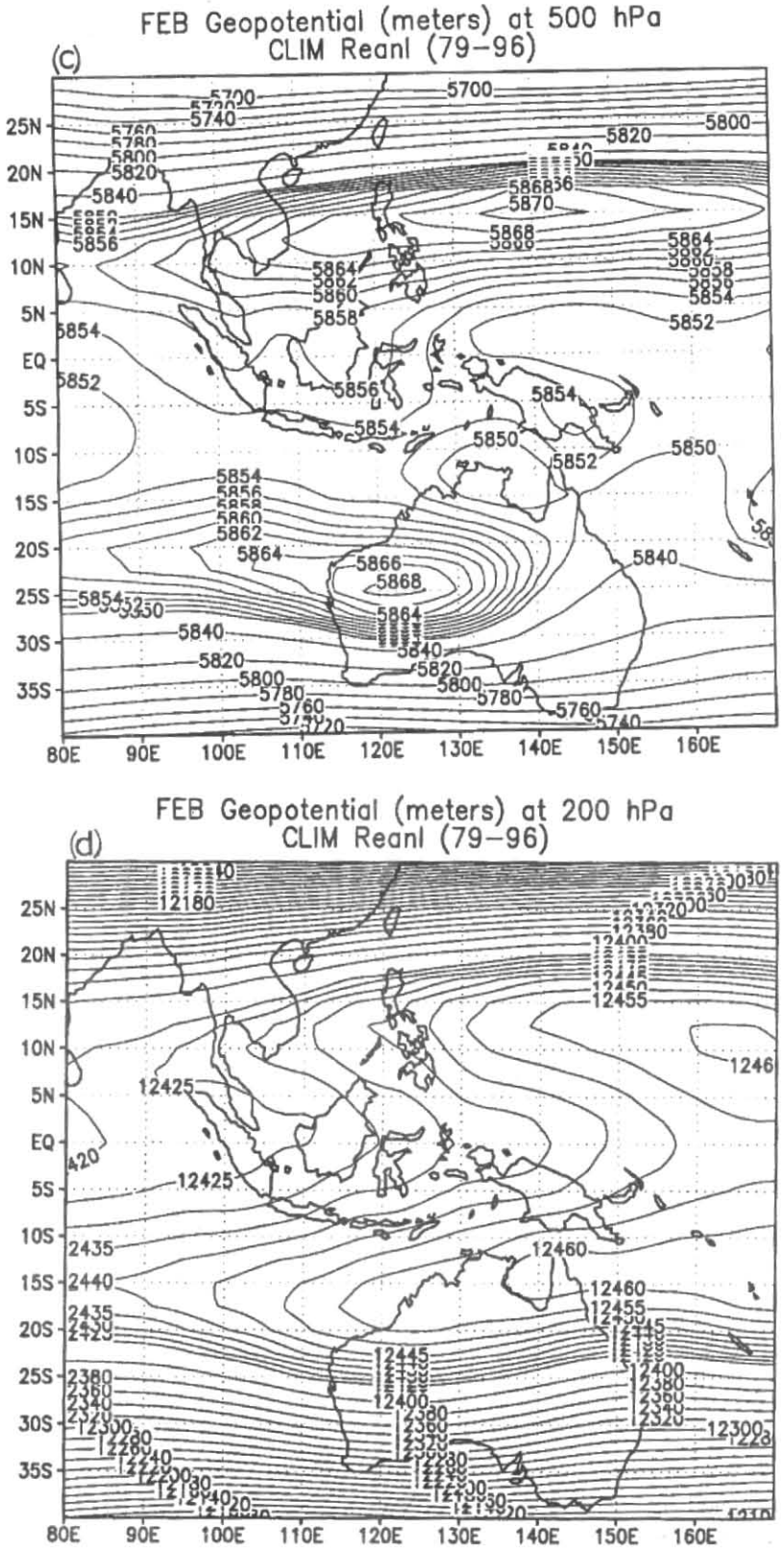

Figs. 2 (c&d). Geopotential height (gpm) fields at 500 and 200 hPa over Australia and surrounding areas

Fig. 1(g) which presents the meridional anomaly (deviation from the meridional mean) of temperature along 125°E, shows that the warmest anomaly near surface along this longitude is located over the Australian continent at a latitude of about 25°S and that its axis tilts equator-ward with height reaching a height of about 4 km over about 15°S. An upper-tropospheric warm anomaly centred over northern Australian between about 10°S and 15°S appears between about 550 hPa and 250 hPa. North of the equator, a strong warm anomaly centred over about 10°N at 650 hPa, appears to overlie a wedge of cold anomaly which appears to be extending from the northern hemisphere subtropics, across the equator, towards the 'heat low' over Australia.

3.2. *MSL – pressure and the geopotential fields*

Figs. 2 (a-d) show the distributions of reanalysis mean sea level pressure and the geo-potential heights of the 925, 500 and 200 hPa pressure surfaces respectively over Australia and the surrounding areas.

Fig. 2(a) shows a closed low pressure area Australia in association with the warmest area over the continent, surrounded by high pressures over the cold oceans. The high pressure to the west appears to be particularly strong because of the coldest anomaly maintained there by the west Australian cold ocean current. The equatorial trough of low pressure runs along about 10°S over the Indian Ocean and 15°S over the Pacific. The pressure field appears to be flat over the equatorial Indian Ocean but a clear north-south gradient is noticeable over the maritime continent which lies to the north of Australia.

The height field at 925 hPa [Fig. 2(b)] appears to be similar to the pressure field at MSL and shows more or less the same features as those at the lower surface. At 500 hPa [Fig. 2(c)], the trough associated with the 'heat low' over Australia appears to be shifted equator-ward with height. At 500 hPa, a well-developed 'high' appears to be located over the central parts of the continent. North of the equator, a 'High' appears over both the Indian and Pacific Oceans with its ridge located between 10°N and 15°N. Cross-equatorial height gradient over the maritime continent, noted at the lower levels, is also noticeable at this surface.

The height field at 200 hPa [Fig. 2 (d)]. Displays two belts of 'high', lying on either side of the equator, with a 'low' in between over the equatorial belt. The ridge of the 'high' in the northern hemisphere lies between 5°N and 10°N over the Indian Ocean and between 10°N and 15°N over the western Pacific, while that in the southern hemisphere runs along about 15°S over both ocean and continent.

3.3. *Wind*

3.3.1. *Wind field at pressure surfaces*

The wind field in and around Australia at 925, 500 and 200 hPa is shown by reanalysis streamline-isotach maps, presented in Figs. 3 (a-c) respectively.

At 925 hPa [Fig. 3(a)], a strong cyclonic circulation (clockwise in the southern hemisphere), apparently associated with the heat low over Australia, is centred near the coast of north-western Australia between about 15°S and 20°S. There is evidence of strong cross-equatorial flow of air from the northern hemisphere subtropical anticyclone to the southern hemisphere 'heat low' circulation, especially over the maritime continent at this surface. There is also evidence of strong divergence of air from the southern-hemisphere subtropical anticyclone located to the south of Australia, which appears to converge into the 'heat low' circulation over the continent.

At 500 hPa [Fig. 3(b)] the ridges of the subtropical anticyclones of the two hemispheres appear to be closer to the equator than at 925 hPa, that of the northern hemisphere being along about 12°N and the southern hemisphere along about 22°S. The cyclonic circulation associated with the ET in the southern hemisphere has its axis along about 12°S.

At 200 hPa [Fig. 3(c)] , the anticylonic circulations associated with the subtropical high pressure belts of the two hemispheres appear to dominate the flow with strong easterlies flowing over the equatorial belt between about 10°N and 15°S and westerlies poleward of this belt in the respective hemispheres.

3.3.2. *Meridional vertical sections*

Fig. 3(d) shows the distribution of the zonal component of the wind in a meridional-vertical section along 125°E which passes through the centre of the 'heat low' circulation at surface over Australia. It shows the approximate domains of the easterly components of the trade-winds of the two hemispheres with the equatorial westerlies in between in the lower troposphere. Aloft, the equatorial easterlies lying between the subtropical westerlies of the two hemispheres dominate the flow. The distribution of the zonal component of the wind, shown in Fig. 3(d), resembles closely that shown earlier by Ramage and Raman (1972), based on the data of the International Indian Ocean Expedition (IIOE), 1963-66, for the month of January and along 140°E. The distribution of the meridional component of the wind along the same vertical section along 125°E is shown in Fig. 3(e). Amongst other

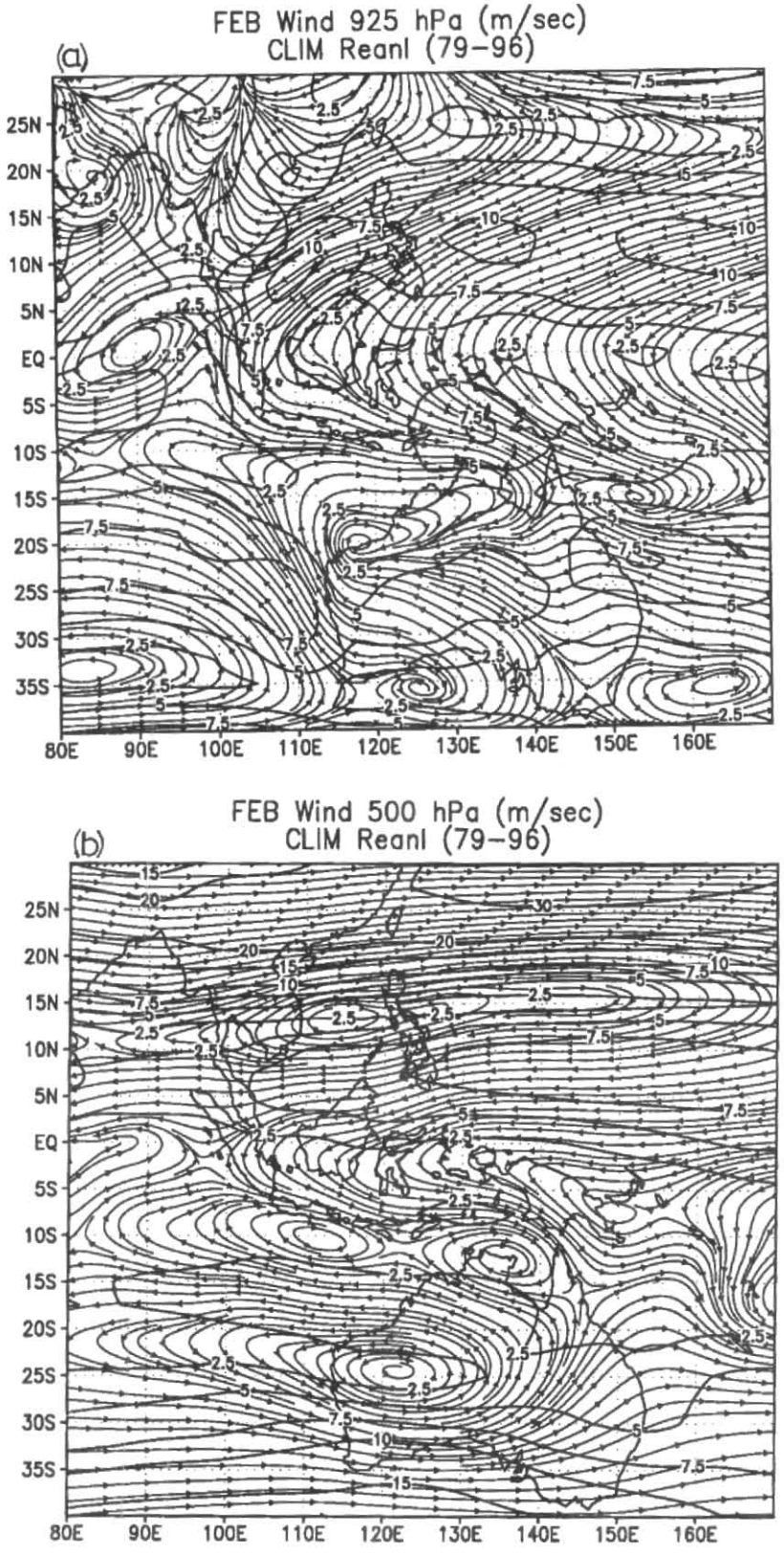

Figs.3 (a&b). Reanalysis wind fields (streamlines and isotachs) over Australia and surrounding regions at 925 and 500 hPa during February

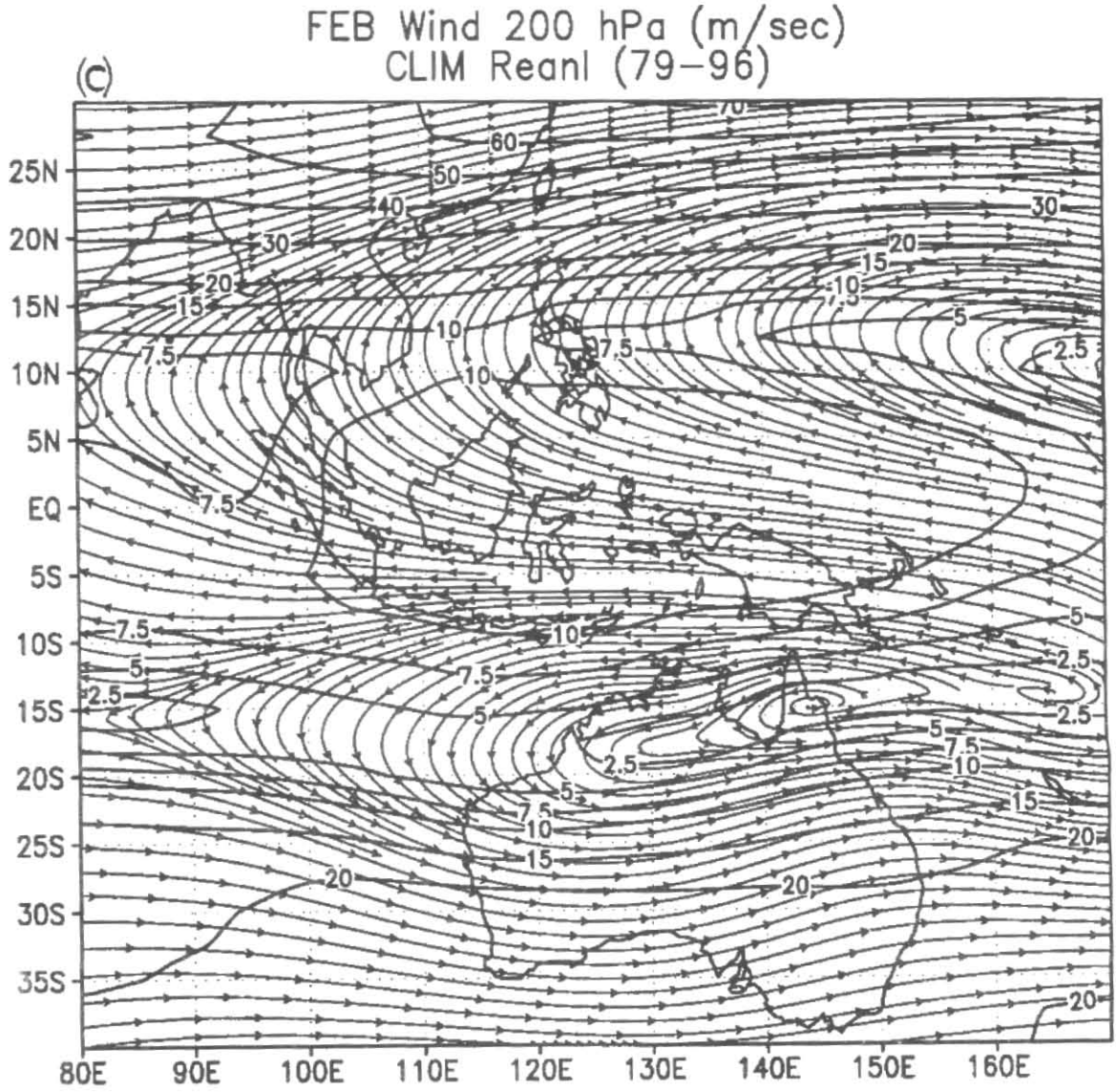

Fig. 3(c). Reanalysis wind fields (streamlines and isotachs) over Australia and surrounding regions at 200 hPa respectively during February

things, it furnishes valuable information on possible inter-hemispheric movements of air at different heights along the selected meridian and their likely zones of convergence and divergence.

3.4. *Specific humidity*

The climatological distribution of moisture in the atmospheric over Australia and neighbouring oceans is brought out by two vertical profiles of specific humidity, one zonal along 25°S [Fig. 4(a)] and the other meridional along 125°E [Fig. 4(b)]. The zonal-vertical profile [Fig. 4(a)] shows concentrations of moisture over the eastern and the western coastal regions and a relatively dry zone in between. The specific humidity is maximum at the lower boundary and falls off with height over both land and sea but over the ocean surface the fall is much more rapid over the Indian Ocean to the west of south-western Australia than over the Pacific to the east of the continent. The meridional-vertical profile along 125°E [Fig. 4(b)] shows large concentrations of moisture over the equatorial belt stretching from about 20°S to about 10°N in the lower troposphere below about 500 hPa. Aloft, the north-south humidity gradient virtually disappears.

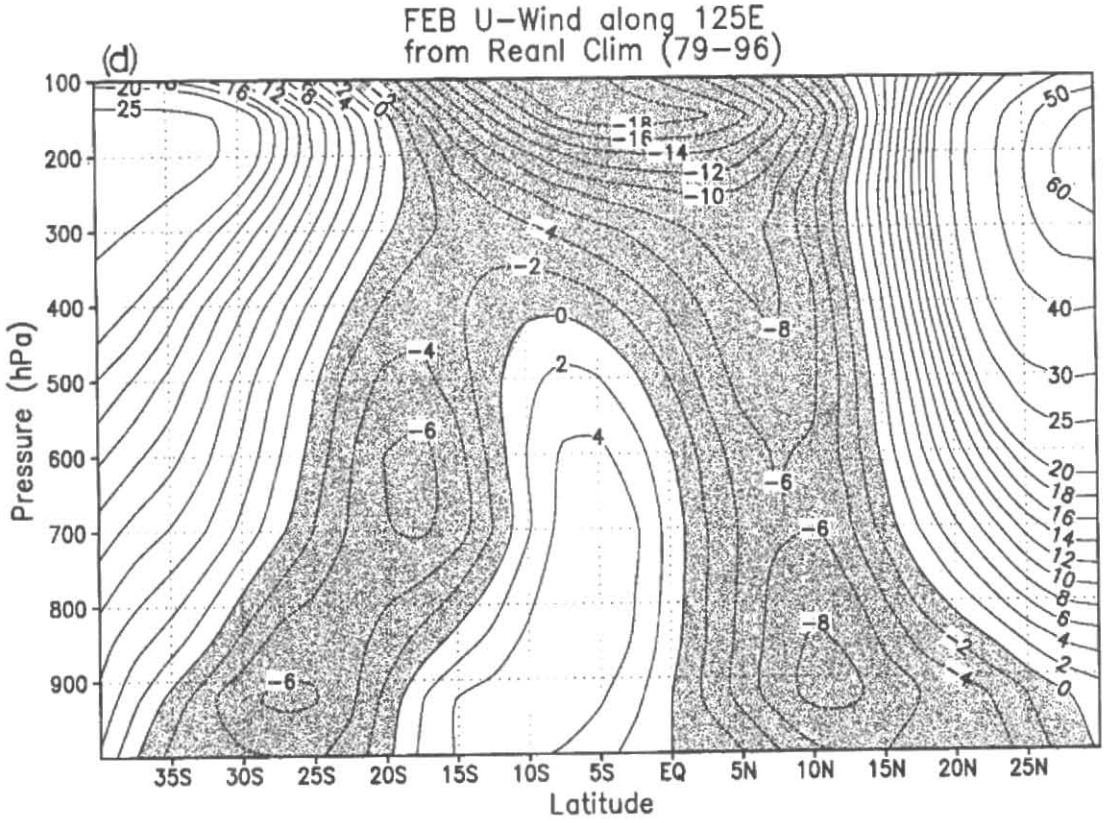

Fig. 3 (d). Vertical distribution of the zonal component of the wind (ms^{-1}) along 125°E . Positive – Westerly, Negative – Easterly

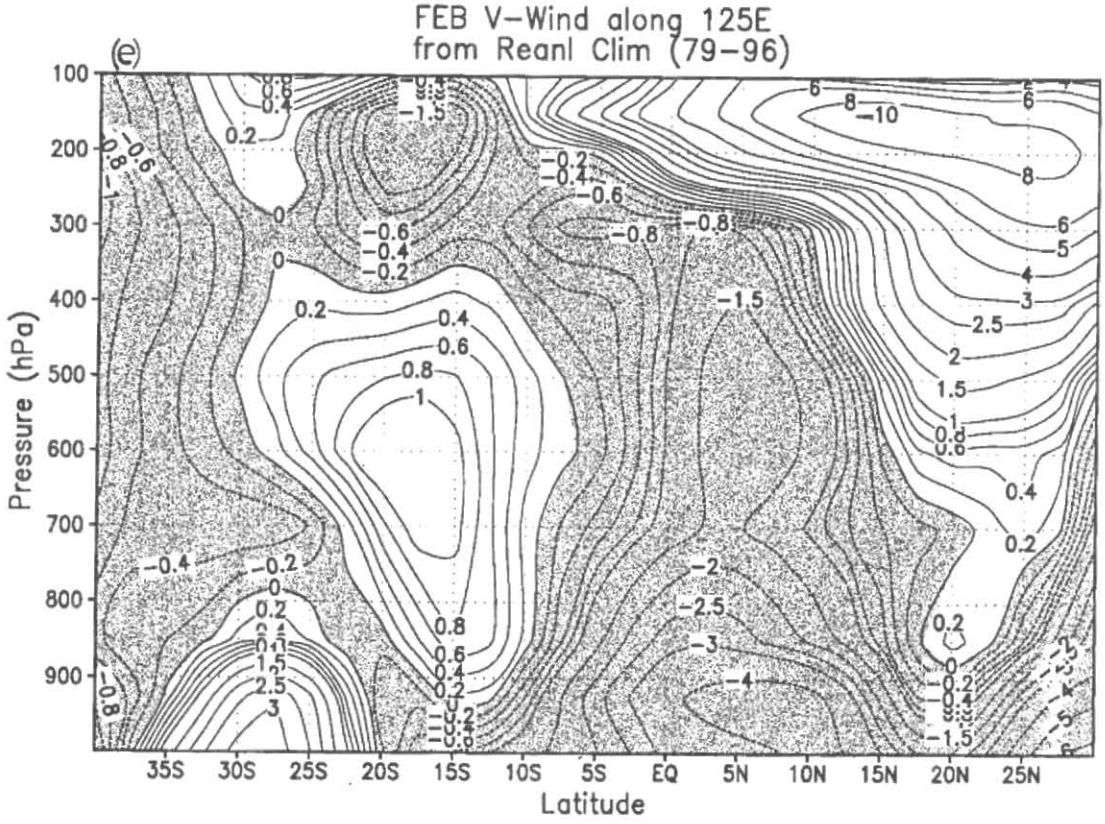

Fig. 3 (e). Vertical distribution of the meridional component of the wind (ms^{-1}) along 125°E . Positive – Southerly, Negative – Northerly

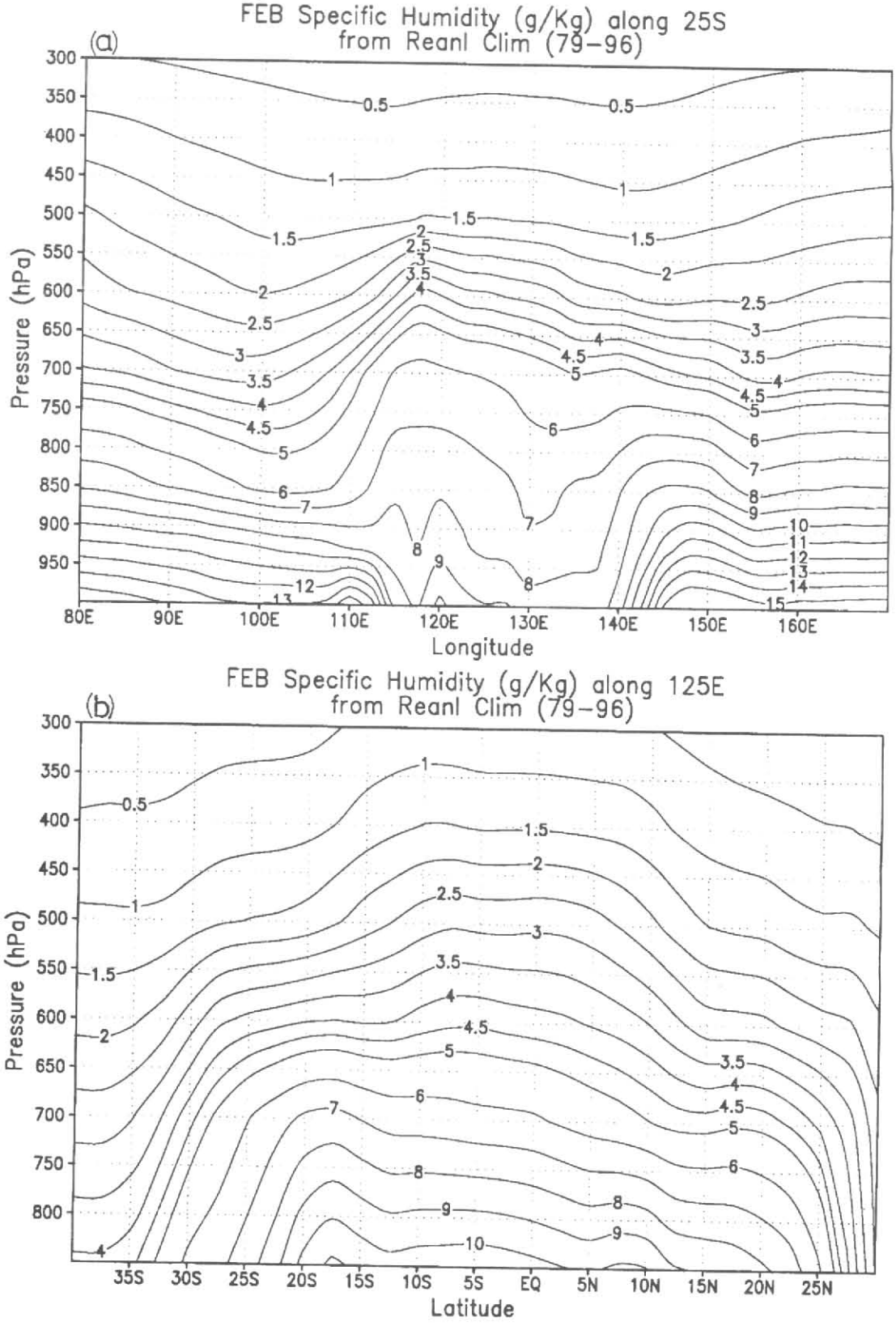

Figs. 4 (a&b). Vertical distributions of specific humidity (g/kg) along: (a) 25°S and (b) 125°E

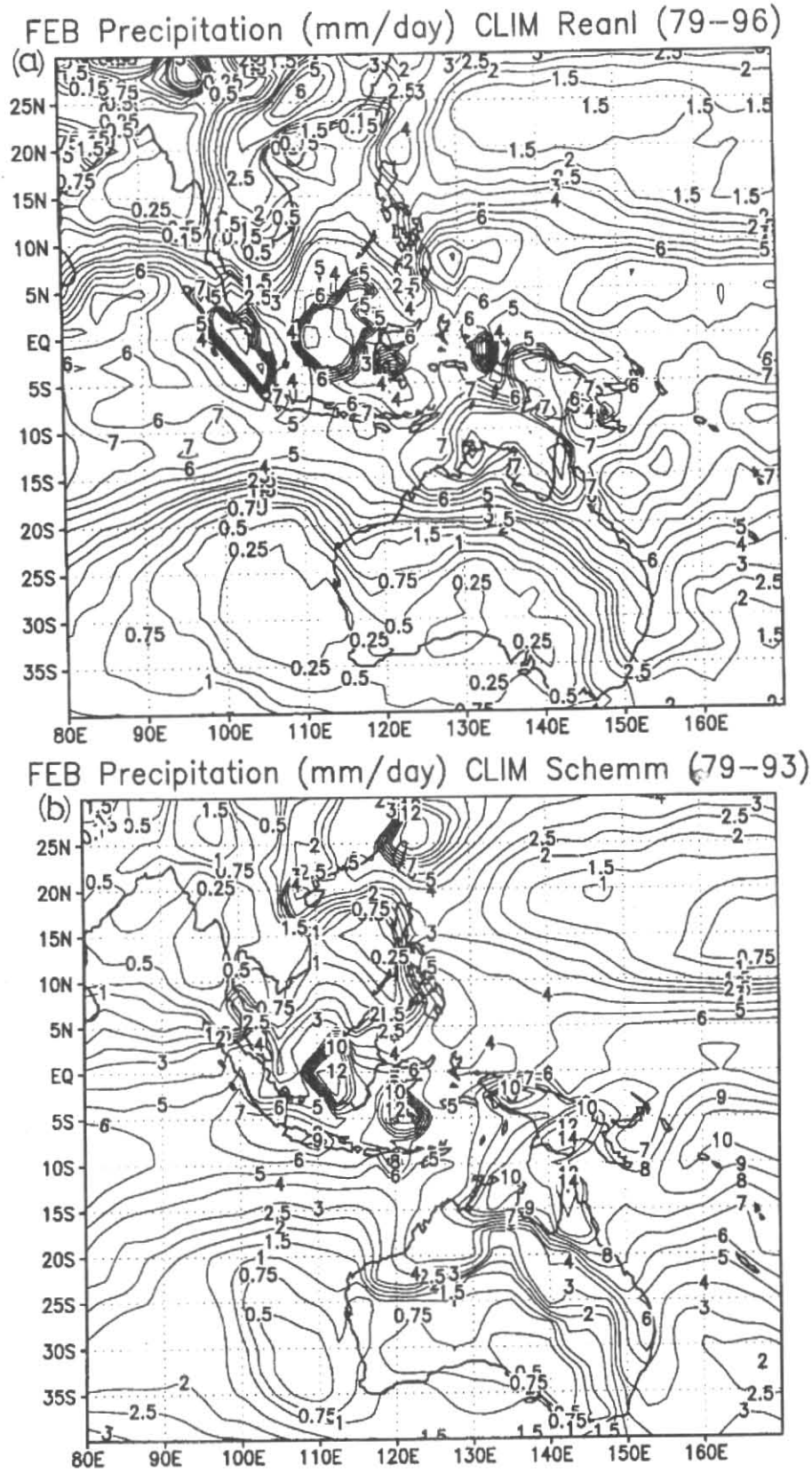

Figs. 5 (a&b). Distribution of February precipitation (mm/day) over Australia and surrounding oceans: (a) Reanalysis, (b) Schemm

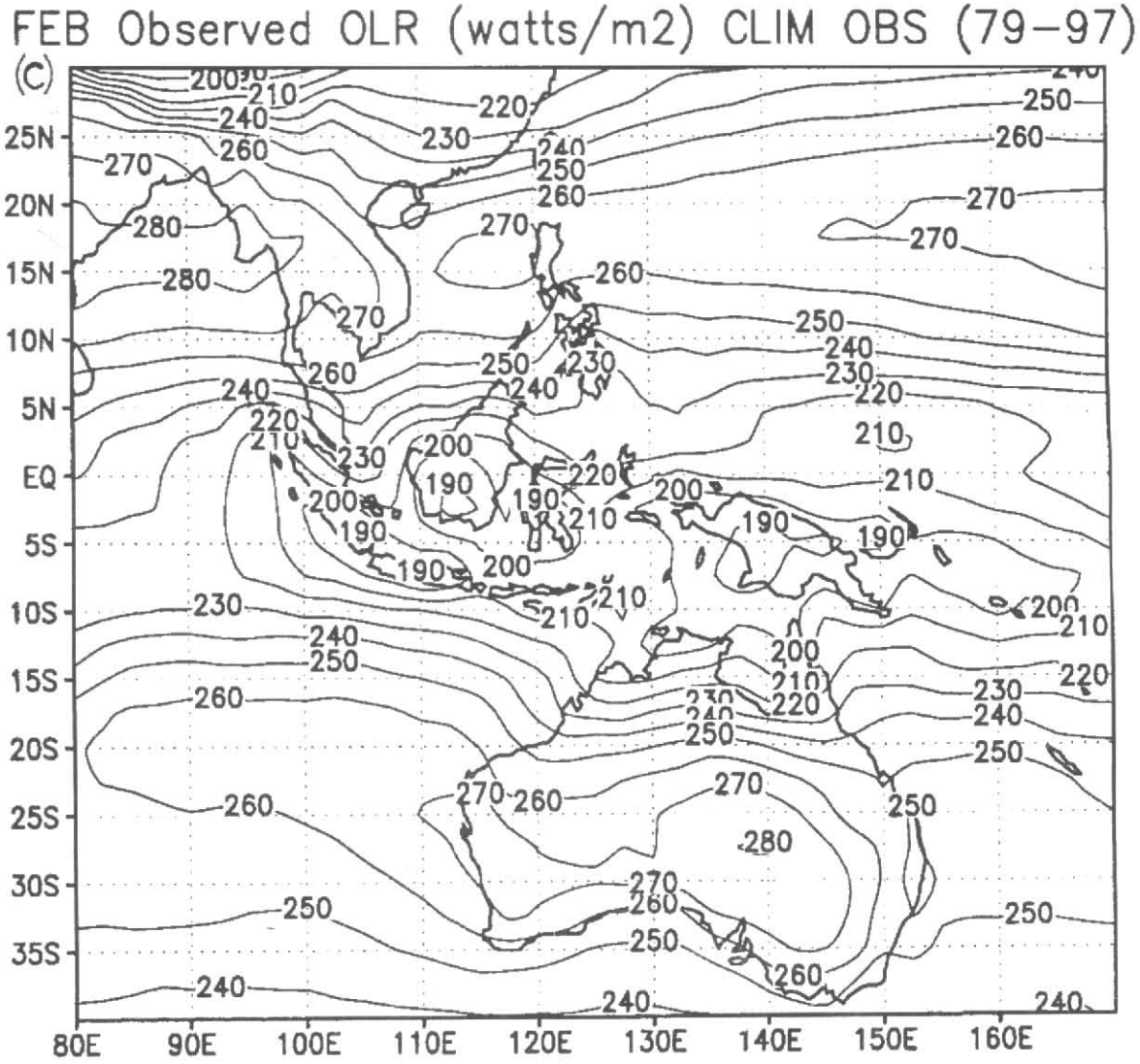

Fig. 5 (c). Field of observed OLR ($W^{-2}m$)

3.5. *Precipitation*

Mean February precipitation over Australia and the surrounding ocean areas, as obtained from reanalysis, is presented in Fig. 5(a). It shows that, over the Australian longitudes, heavy rain exceeding 6.0 mm/day is concentrated over the northern and northeastern parts of Australia and adjoining oceanic areas and the Maritime continent extending northward to about 15°N. Across Australia, the rainfall rate decreases rapidly towards the south, reaching a value less than 0.25 mm/day over the coast of southern Australia. Zonally, there appears to be a sharp contrast in the rate of rainfall between the east and the west coasts of southern Australia. Along the coast of New South Wales, for example, rainfall exceeds 4-5 mm/day, whereas that near the coast of western Australia, in almost the same latitudinal belt, hardly reaches 0.25 mm/day. A vast area of the southern Indian ocean extending westward from the coast of southwestern Australia to about 80°E appears to have very little rain (less than 1.5 mm/day). However, to the north of this dry area, a belt of heavy rain exceeding 6 to 8 mm/day appears around 10°S in association with the location of the ET/ITCZ south of the equator. Equatorward of this rainy belt, rainfall appears to decrease somewhat but increase again to reach a maximum of about 8 mm/day a few degrees north of the equator over the Bay of Bengal. Here, in the meridional profiles of rainfall across the equatorial eastern Indian ocean, one can see some evidence of two equatorial troughs, one on either side of

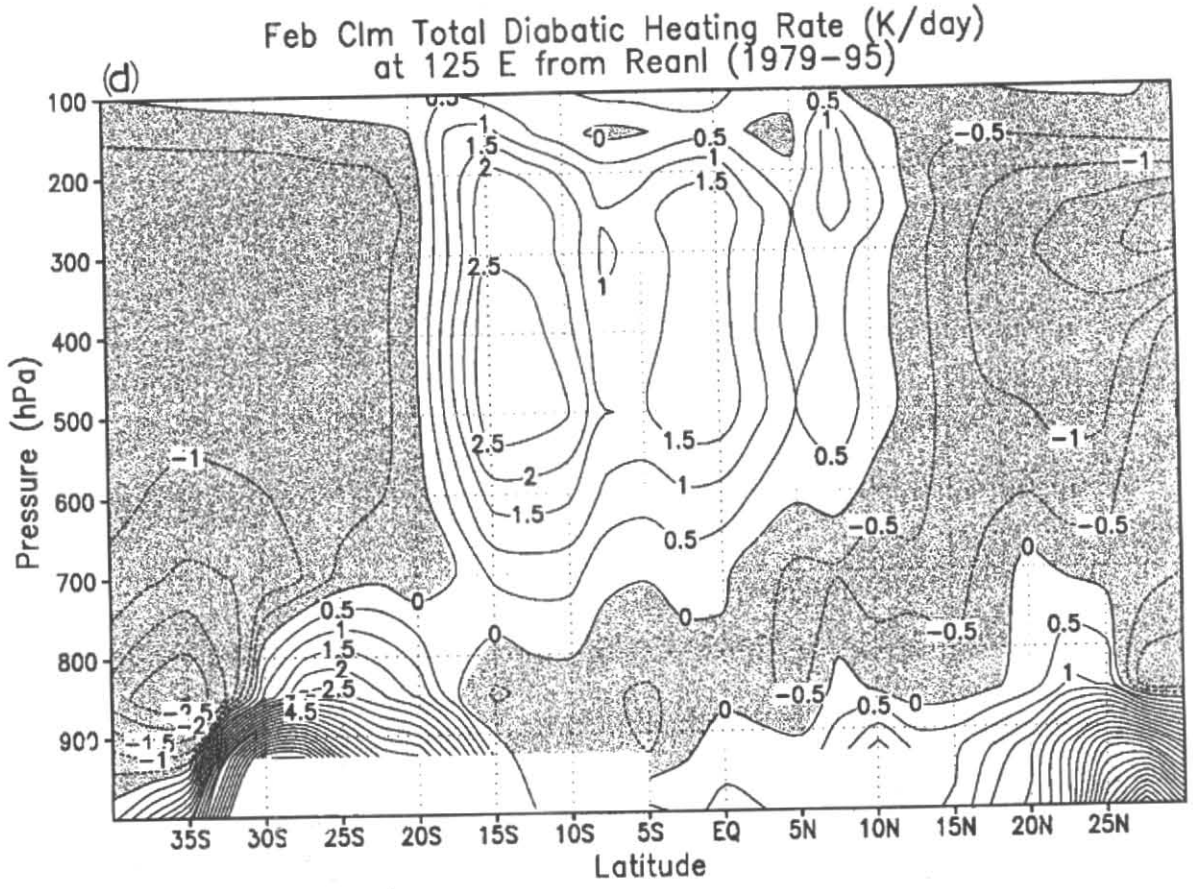

Fig. 5 (d). Meridional-vertical distribution of total diabatic heating rate along 125°E

the equator, suggested earlier by several workers (*e.g.* Raman, 1965; Saha, 1973). A very similar situation appears to exist over the equatorial western Pacific where two heavy rainfall belts appear, one on each side of the equator.

It is difficult to assess the reliability of the distribution of the model-derived rainfall described above, especially over the ocean areas surrounding Australia, but several observed climatological rainfall datasets (*e.g.*, Xie and Arkin, 1996) are available to compare the model rainfall climatology with. In the present study, an observed precipitation dataset for period, 1979-93, prepared by J.-K.E. Scheme at NCEP is used and shown in Fig. 5(b). Schemm's precipitation climatology was generated by merging observed monthly total precipitation data from surface station networks all over the world with estimated oceanic precipitation from the MSU measurements (Spencer, 1993), following a procedure explained in Schemm *et al.*, (1992). In this procedure, station data reporting rainfall amounts exceeding 1000 mm were ignored. To remove sea ice contamination in regions poleward of 50 degree latitude, the MSU estimates with monthly totals greater than 900 mm were also ignored. A comparison of the reanalysis precipitation with Schemm's observed precipitation climatology shows a large measure of agreement between the two. For example, areas of heavy rainfall over the northern and eastern parts of Australia as well as those of low rainfall over the southern parts of the continent stand out in both the climatologies. Likewise, the exceedingly dry area over the Indian ocean to the west of southwestern Australia appear in both the climatologies. The field of reanalysis precipitation also appears to be in substantial agreement with those of the Outgoing Longwave Radiation (OLR) and Total Diabatic Heating shown in Figs. 5(c&d) respectively. In general, low values of OLR and net high positive values of diabatic heating in the middle and upper troposphere appear to correlate well with regions of heavy precipitation.

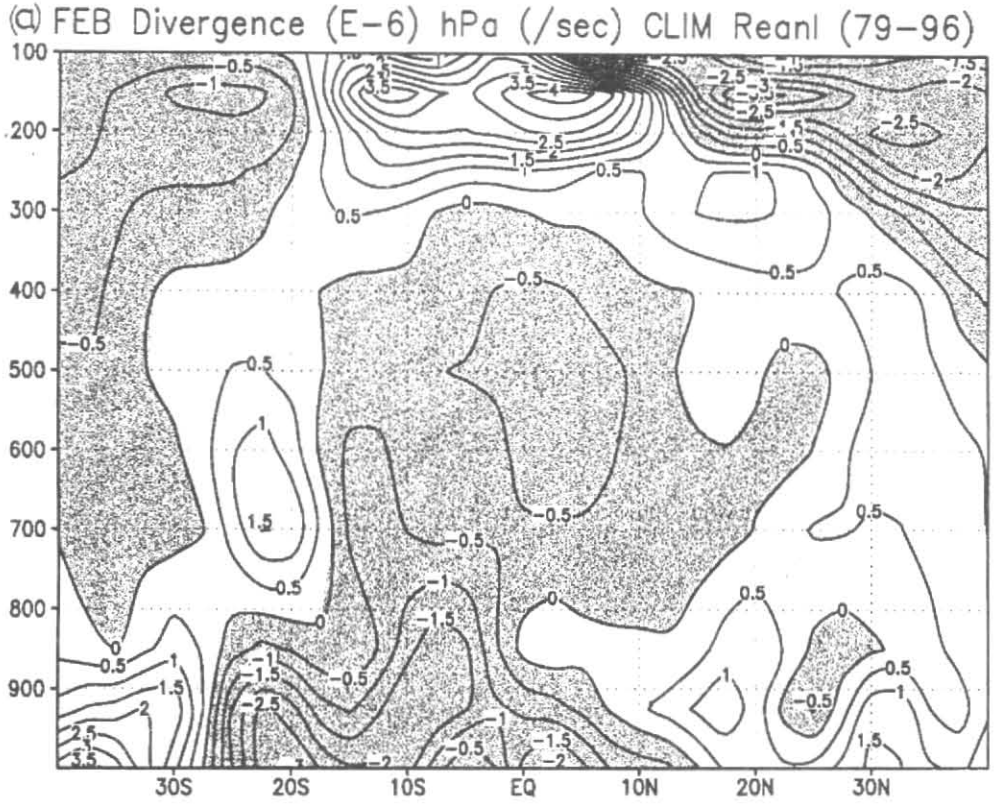

Fig. 6 (a). A meridional-vertical section (zonally averaged over longitudes, 105°E - 150°E) showing the distribution of Divergence (unit: 10^{-6} s^{-1}) during February

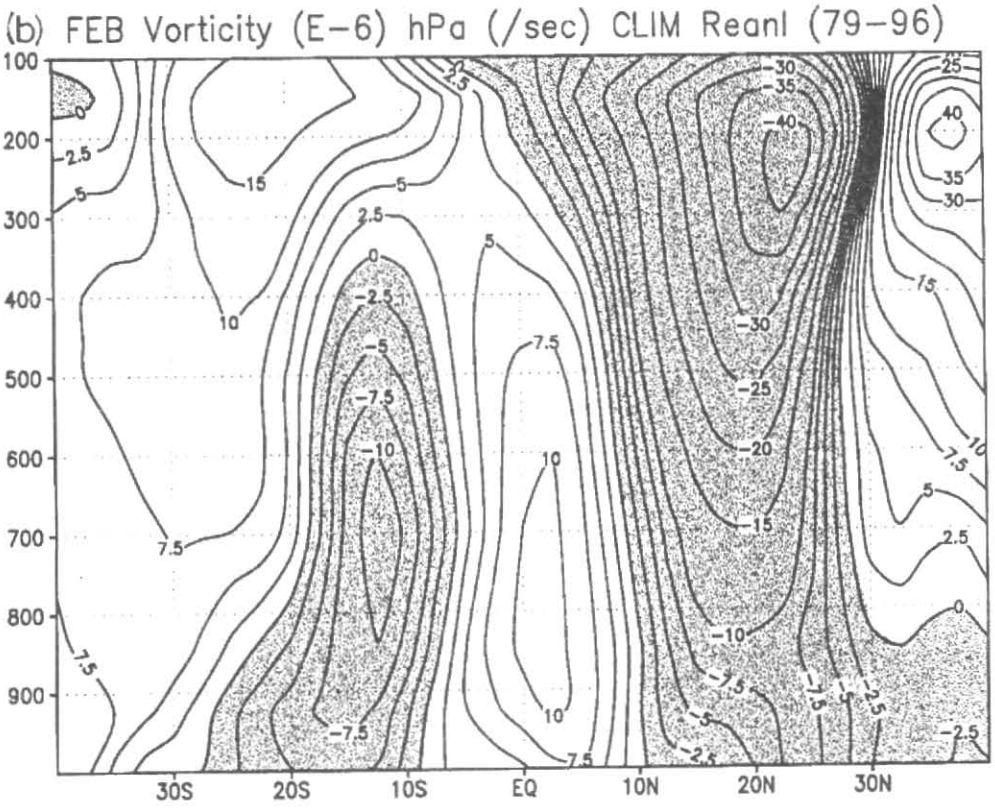

Fig. 6 (b). Same as in Fig. 6a, but for relative vorticity

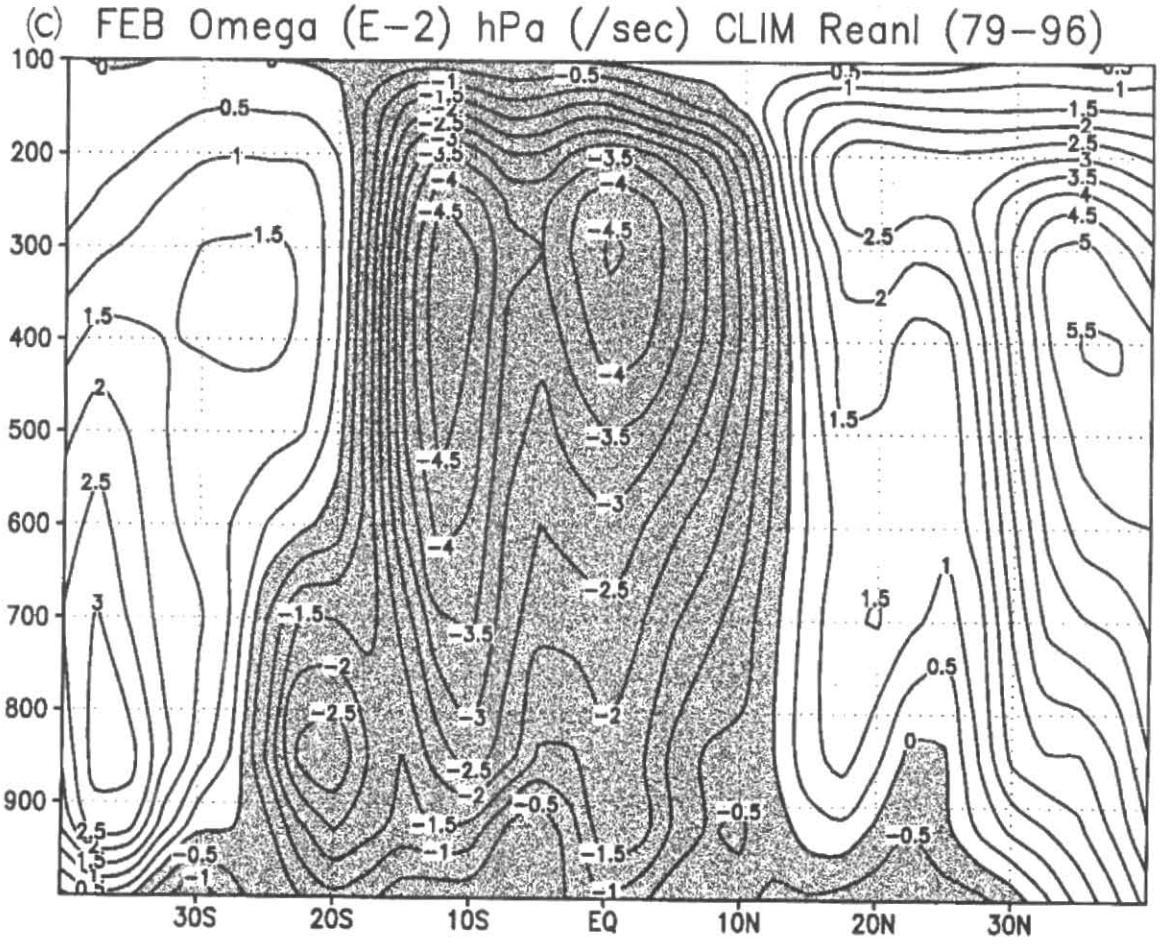

Fig. 6 (c). Same as in Fig. 6a, but for omega (unit: 10^{-2} hPa s^{-1})

4. Fields of divergence, vorticity and vertical motion

A knowledge of the climatological distributions of some of the derived parameters of the wind, such as divergence, vorticity and vertical motion, is essential for understanding atmospheric circulation in any region and assessing its impact on the weather and climate of the region. Therefore, in what follows, we present the distribution of these parameters in a meridional-vertical section through Australia by zonally averaging their values between longitudes 105°E and 150°E. The findings are as follows :

4.1. *Divergence*

Fig. 6(a) shows the north-south distribution of the zonally-averaged values of mean February divergence, the broad patterns of which appear to be as follows :

(*i*) In the lower troposphere below about 800 hPa, with a little exception in the northern hemisphere, two areas of fairly strong divergence appear, one in the southern hemisphere south of about 25°S and the other in the northern hemisphere north of about 10°N with an extensive area of strong convergence in between. It is noteworthy that the strongest convergence in this layer is located in the southern hemisphere between about 15°S and 25°S. Another noticeable feature of the distribution is that the surface separating the areas of divergence and convergence in each hemisphere appear to be tilted equatorward with height.

(*ii*) In the layer between about 800 hPa and 350 hPa, the hemispheric patterns appear to be quite different. In the southern hemisphere, strong divergence appears almost directly above low-level convergence between about 25°S and 15°S, whereas convergence appears above low-level divergence south of this latitudinal belt. In the equatorial belt extending from about 15°S

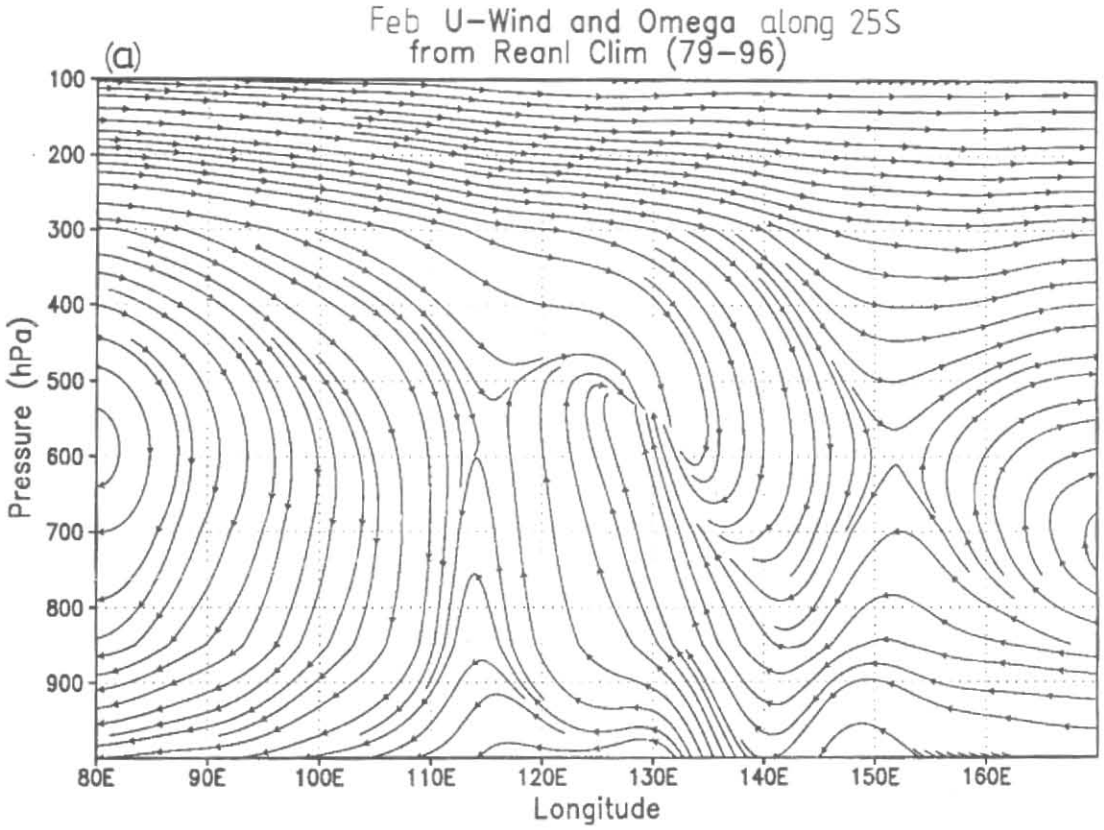

Fig. 7 (a). A zonal-vertical section showing resultant streamlines (constructed from the zonal and the vertical components of the wind) along 25°S during February

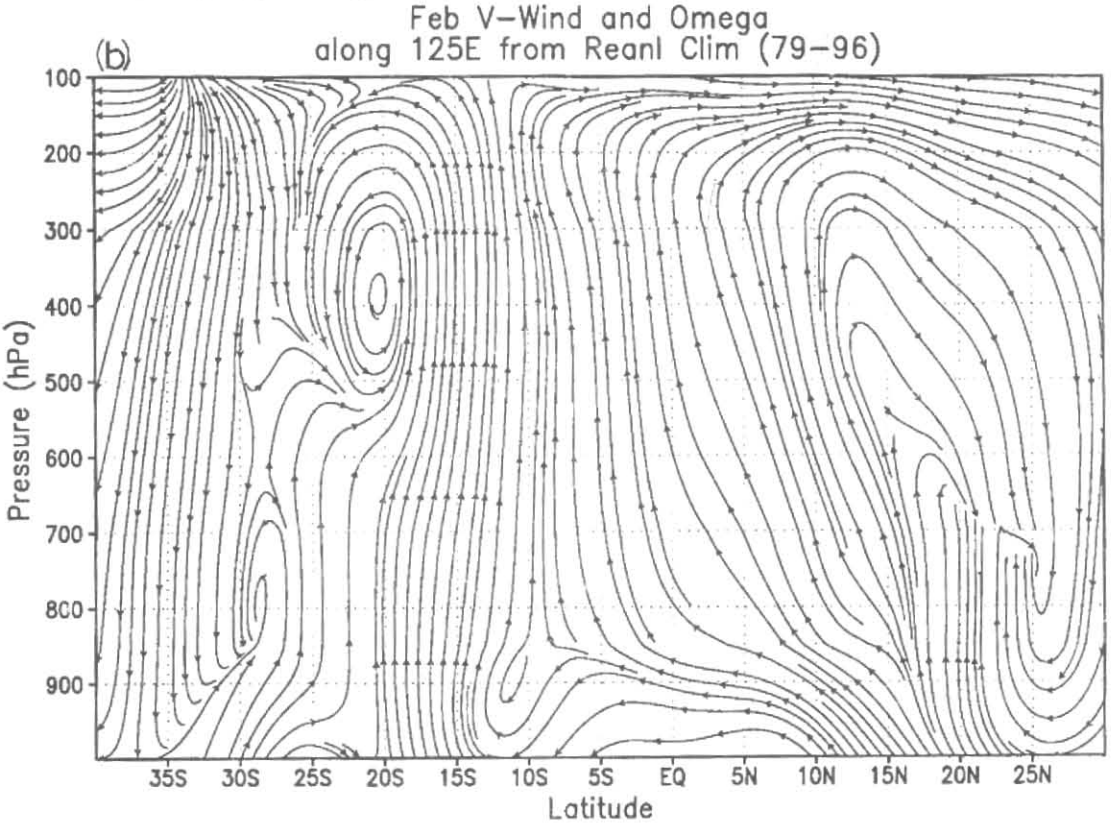

Fig. 7 (b). A meridional-vertical section showing resultant streamlines (constructed from the meridional and the vertical components of the wind) along 125°E during February

to the equator, a deep layer of convergence appears extending from sea level to the top of this layer. In the northern hemisphere, a broad area of convergence between the equator and about 15°N has divergence to its north.

(*iii*) In the upper troposphere above about 300 hPa, strong divergence appears over the equatorial belt between about 15°S and 15°N with convergence poleward of this belt in both the hemisphere.

4.2 *Vorticity*

The meridional-vertical distribution of mean February relative vorticity, presented in Fig. 6(b), shows, after taking due congnizance of change of sign of relative vorticity in the southern hemisphere, the following :

(*i*) Below about 350 hPa, there are two prominent belts of positive relative vorticity, one in the northern hemisphere with maximum located between the equator and 10°N and the other in the southern hemisphere with maximum located at surface near about 20°S but tilting equatorward with height upto about 700 hPa. Poleward of the belt of positive relative vorticity in each hemisphere, relative vorticity becomes negative. However, in the northern hemisphere, relative vorticity north of about 30°N becomes positive above about 800 hPa.

(*ii*) In the upper troposphere, above about 350 hPa, the relative vorticity is largely negative with maxima located over the subtropical belts of both the hemispheres.

4.3. *Vertical motion (Omega field)*

The meridional-vertical cross-section through the February Omega field, presented in [Fig. 6(c)] shows a wide inter-hemispheric zone of upward motion extending from about 25°S to about 12°N. Within this zone, three distinct cells are identifiable, one with strong low-level convection centred at about 20°S, the second with penetrative convection near about 10°S and the third also with penetrative convection in the vicinity of the equator. The vertical motion is clearly downward poleward of this zone in north the hemispheres.

5. Vertical circulations –Zonal/meridional

By combining vertical motion with the zonal or the meridional component of the wind, one could construct approximate resultant streamlines in zonal-vertical or meridional-vertical planes along selected latitudes or longitudes and study the upward or downward motions of the zonal or the meridional aircurrents (*e.g.*, Saha and Saha, 1993). Vertical circulations of this kind utilising the divergent u or v components of the wind and vertical motion along selected latitudes or longitudes are now routinely published every month by the Climate Diagnostics Bulletin of the U.S.A. In the present study, we show in Figs. 7(a &b) a zonal-vertical circulation along 25°S and a meridional-vertical circulation along 125°E respectively, both of which pass through the approximate centre of the heat low at surface over Australia. The circulation features shown by Fig. 7(a) may be described as follows: Below about 600 hPa, the easterly tradewinds from the Pacific rise over the Great Dividing Range, then subside over the plains of eastern Australia, but rise again over the western part (west of about 140°E) to attain a height at about 500 hPa over the coastal belt of western Australia. However, the off-shore winds descend steeply over the neighbouring cold ocean where the upper-tropospheric westerlies also descend steeply in a clockwise circulation. Indeed, the upper-tropospheric westerlies descend over most parts of Australia along this latitude but nowhere is this descent more striking than the region between about 125°E and 145°E, which is known to be the dry and desert region of the continent. The meridional-vertical circulation, presented in Fig. 7(b), shows two oppositely-circulating, deep and dominant circulation cells, one in each hemisphere, with their rising branches on the equatorward side of their centres, and a lower-tropospheric feeble circulation cell over Australia. It is obvious that the two circulation cells are the well-known Hadley cells of the two hemispheres and the latter is associated with the monsoon circulation over the Australian continent. The two Hadley circulations appear to differ significantly in their character and spatial location. That in the northern hemisphere is much larger in dimensions, both latitudinally and vertically than its counterpart in the southern hemisphere. In fact, the northern-hemispheric Hadley cell which appears to be centred rather close to the equator penetrates deep into the southern hemisphere upto about 15°S to meet its counterpart of the southern hemisphere and the monsoon circulation cell over the Australian continent. Vertically, the Hadley cell of the southern hemisphere is lifted by the monsoon cell so as to have its descending branch above the heat low and its ascending branch to merge with the ascending branches associated with the monsoon trough and the northern hemispheric Hadley cell. Thus, penetrative convection occurs over a broad belt of latitudes extending on either side of the equator. Keeping in view the distributions of moisture and vertical motion, presented in the preceding sections, the vertical circulations shown in Figs. 7(a &b) would seem to have important implications for weather and climate over the region. It is the deep moist

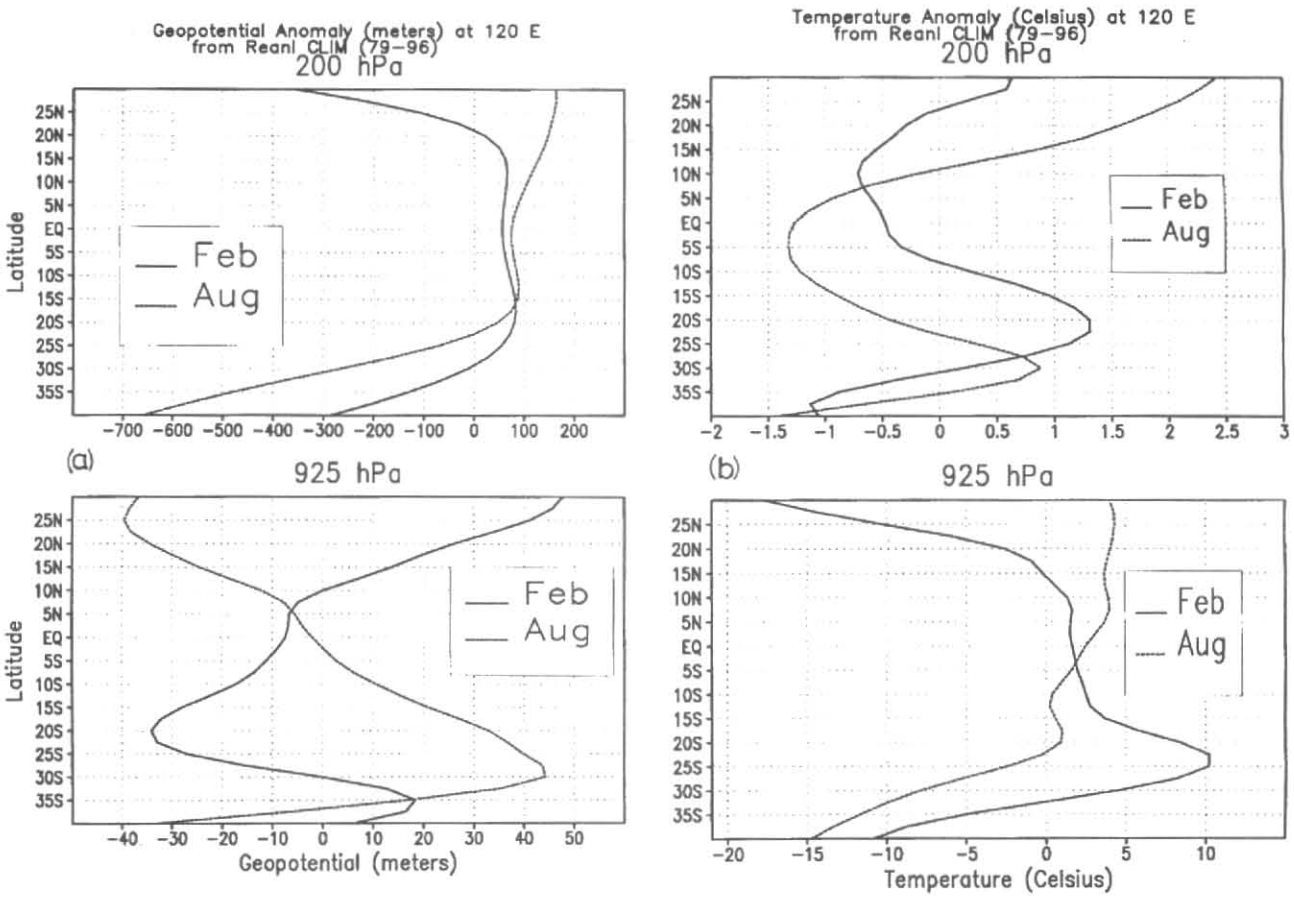

Figs. 8 (a&b). Meridional profiles along 120°E at 925 hPa and 200 hPa during February and August. (a) geopotential height anomaly, and (b) temperature anomaly

convection in the equatorial trough zone that must be associated with the observed heavy rainfall over the northern part of the containent. Earlier, Davidson *et al.* (1983, 1984) who studied the distribution of divergence and the divergent component of the wind at 950 and 200 hPa had alsos inferred that monsoon convection occurred in the upward branches of two linked Hadley circulations, one from each hemisphere, and that the initiation of this convection coincided with the onset of summer monsoon over Australia.

6. The Asian connection – seasonal reversals

The Australian summer monsoon has often been described as being similar to its counterpart in the northern hemisphere (*e.g.,* Davindson *et al.,* 1983) in that both are caused by land-sea thermal contrast and both have equatorial westerlies on the low-latitude side of their equatorial or monsoon troughs. However, seasonally, they are almost 180 degrees out of phase. This would be clear from Figs. 8(a & b) which show the February and August distributions of meridional anomaly (deviation from the meridional mean) of geopotential height and temperature respectively at 925 and 200 hPa along 120°E, a longitude that passes through the extreme western (eastern) part of Australia (Asia). Both would seem to highlight a see-saw relationship between the two continents. In the geopotential field, at 925 hPa, Australia has a low and Asia a high in February but the role is reversed in August when Australia has a high and Asia a low. There appears to be a distinct gradient of geopotential height from one continent to the other in both the months. At 200 hPa, the connection between the continents does not appear to be so obvious as at the low-level, perhaps, because of the vertical reversal of pressure with height as well as the general north-south movement of the pressure belts following the seasonal movement of the sun. At 200 hPa, two highs are poised on either side of the equator but that over the summer continent appears to be the stronger. The see-saw relationship between the

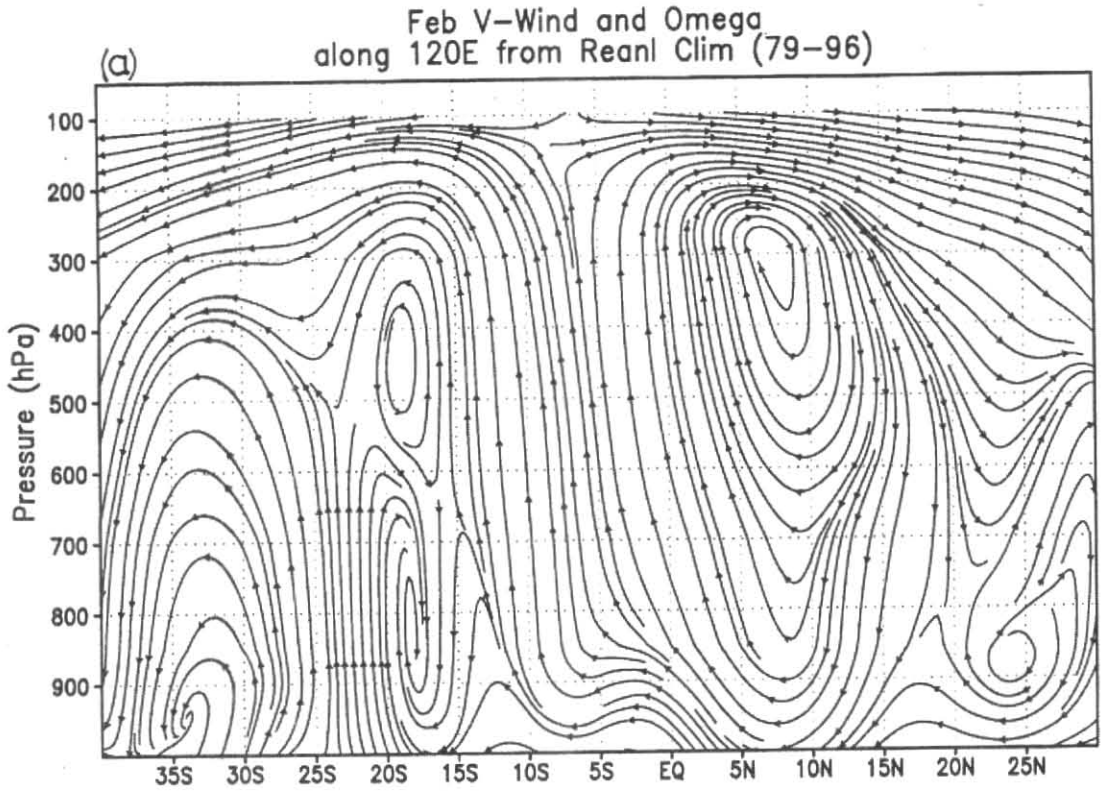

Fig. 9 (a). Meridional-vertical circulations along 120°E during February

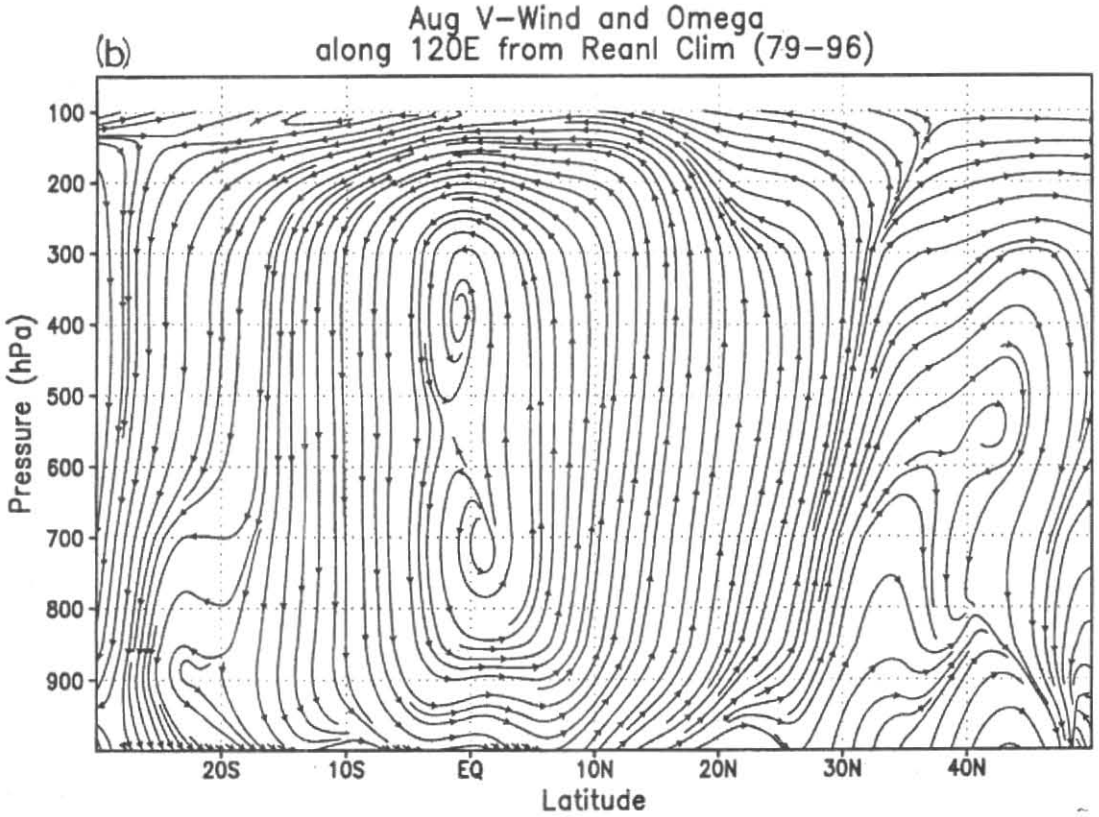

Fig. 9 (b). Meridional-vertical circulations along 120°E during August

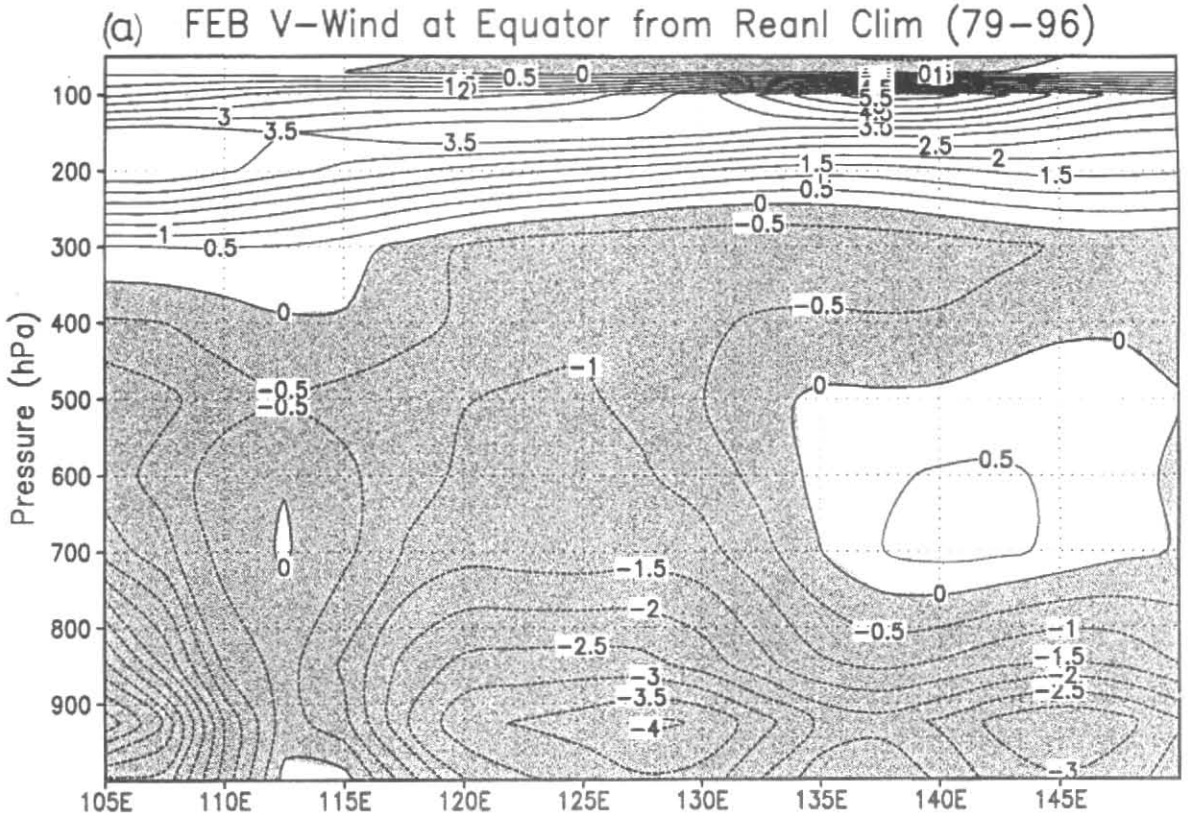

Fig. 10 (a). Vertical distribution of the meridional component of the wind (ms^{-1}) along the equator from 105°E to 150°E during February

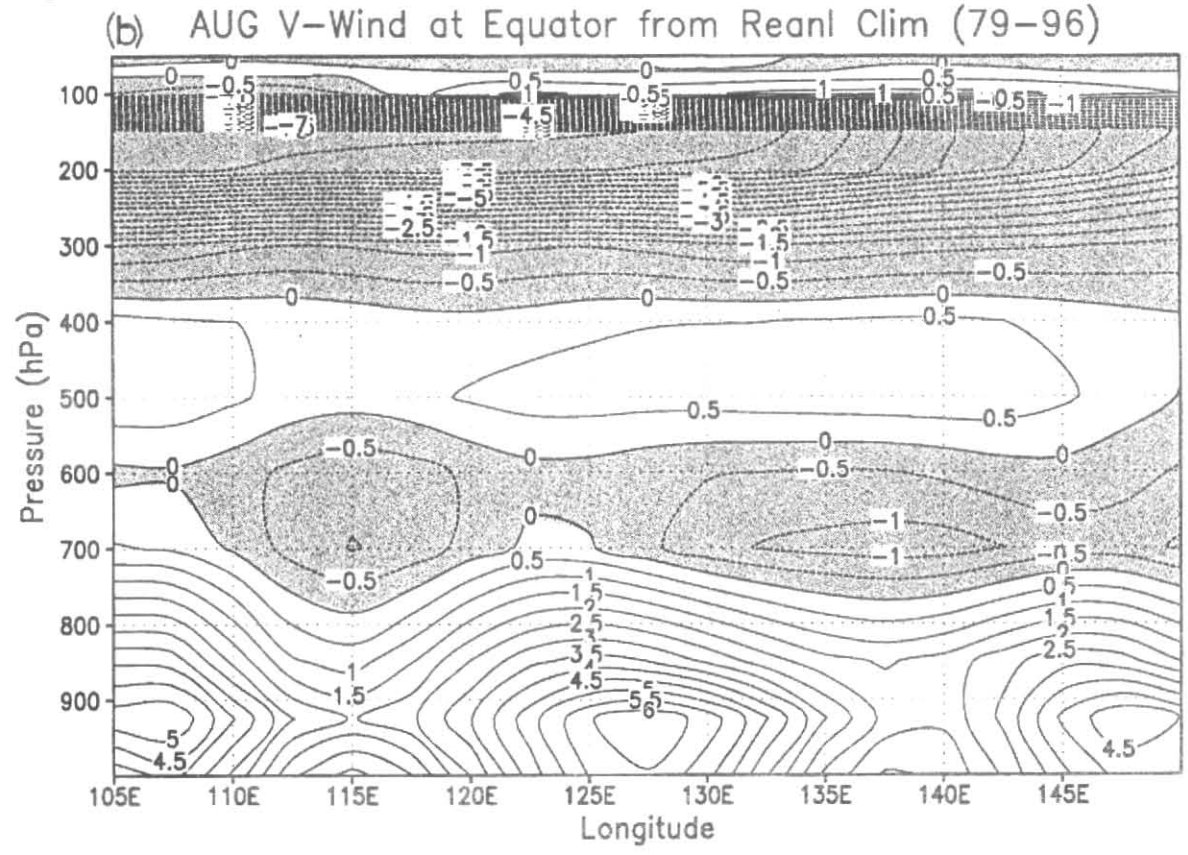

Fig. 10 (b). Vertical distribution of the meridional component of the wind (ms^{-1}) along the equator from 105°E to 150°E during August

TABLE 1

Magnitude of estimated and computed cross-equatorial fluxes of air [Unit : 10^{12} metric tons (day $^{-1}$)]

	Layer	January/ February	July/August
Estimated total across the whole equator (Rao)	Lower	-18.49	16.20
Western Indian ocean (Findlater)	Do	-2.28	7.68
Western Indian ocean (Saha)	Do	-	5.03
Australian section (Present study)	Do	-3.14	2.68
	Upper	1.93	-4.00

two continents is also reflected in the meridional profiles of temperature anomalies presented in Fig. 8 (b). A perceptible gradient of temperature exists across the equator from the warm to the cold continent in both February and August. The Asian connection of the Australian monsoon is also well reflected in the vertical circulations along 120°E, presented in Figs. 9 (a & b).for February and August respectively. One may note some differences between Fig. 9 (a) and Fig. 7 (b) both for February, in the locations of the Hadley and monsoon cells. It is likely that different land-sea configurations along the two chosen longitudes may be responsible for these differences. However, Fig. 9 (a&b) would seem to bring out the seasonal give-and-take relationship between the two continents in the lower and the upper tropospheres. This relationship is particularly evidenced in the lifting of the Hadley cell by the Monsoon cell to the middle and upper troposphere in the summer hemisphere and the disappearance of the monsoon cell and the descent of the Hadley cell to the MSL in the winter hemisphere.

7. Cross-equatorial fluxes of air

One of the first to estimate mean interhemispheric fluxes of air using data within a strip of latitude between 5°N and 5°S around the globe was Rao (1964) who found that, on an average, the quantity of air that crosses the equator in the lower troposphere, using a unit of 10^{12} m. tons $(day)^{-1}$, is –18.49 in January and 16.20 in July. Findlater (1969) who computed the fluxes of air across an equatorial section extending from 35°E to 75°E and from surface to 400 hPa in the western Indian ocean found, using the same units, a value of – 2.28 in January and 7.68 in July. For an equatorial-vertical section over the same ocean, extending from 42°E to 75°E and from surface to 450 hPa, Saha (1970), using the data of the International Indian Ocean Expedition in July 1964, found a northward flux of 5.03 in the same units. To the knowledge of the authors, no such computation of cross-equatorial fluxes of air in different seasons appears to have been carried out in the Australian monsoon region, although several workers (*e.g.,* Murakami and Sumi, 1982; Davidson *et al.*, 1983 and 1984; Tao and Chen, 1987) have noted the existence of such flows and dwelt on their importance in the context of the monsoon circulations over Asia and Australia. Tao and Chen (1987), who used the data of the Summer Monsoon Experiment over the Indian ocean and western Pacific in July 1979, computed the meridional component of the wind along an equatorial section extending from 0° to 180°E and showed that in the segment between about 100°E and 150°E, strong southerlies crossed the equator in the lower troposphere and northerlies in the upper troposphere. In the present study, using the meridional component of the wind shown in Figs. 10 (a &b)] from reanalysis for February and August respectively, the authors computed the interhemispheric transport of air across an equatorial section from 105°E to 150°E for the lower troposphere (surface to 300 hPa) and the upper troposphere (300 to 50 hPa). The results showed that in February the total cross-equatorial flux was –3.14 units in the lower troposphere and 1.93 in the upper troposphere.

The corresponding figures in August were 2.68 and – 4.00. A comparative statement of the estimated cross-equatorial fluxes of air around the globe and those computed over the western Indian ocean section and the Australian section is presented in Table 1.

Table 1 testifies that while during the Asian summer the lower-tropospheric cross-equatorial flux is northward over both the western Indian ocean and the Australian sections, that over the former is almost three times that over the latter. The relative importance of the two sections, however, changes during the Australian summer in February. The low-level southward flux across the equator in the Australian sector then exceeds that over the western Indian ocean sector by almost 40 per cent. Table 1 also shows that in the Australian section, the lower and upper-tropospheric cross-equatorial fluxes in any season are in opposite directions and their magnitudes differ from each other.

8. Summary and conclusion

By design, the scope of the present study (Part 1) has been limited to provide a general description of the time-mean meteorological fields associated with the observed weather and climate of Australia, as revealed by reanalysis. The horizontal and vertical profiles of several variables, such as temperature, pressure, geo-potential heights, winds and humidity as well as distributions of such derived parameters as divergence, vorticity, vertical motion and precipitation appear to suggest a see-saw or give-and-take relationship between the continents of Australia and Asia in both Austral summer and winter. Indeed, there appears to be a redistribution of atmospheric mass between the two continents situated on either side of the equator between the seasons. In any season, mass appears to diverge from the winter to the summer hemisphere in the lower troposphere and return from the summer to the winter hemisphere in the upper troposphere, to complete an interhemispheric circulation. A seasonal redistribution of mass of this kind between two hemispheres was postulated by Van den Dool and Saha (1993). Cross-equatorial fluxes computed for the Australian sector show that during Australian summer, the magnitude of the low-level flux from Asia to Australia is larger than that of the upper-air flux in the opposite direction whereas, during Australian winter, the magnitude of the low-level flux from Australia to Asia is smaller than that of the upper-air flux from Asia to Australia.

In part 2 of the study, the authors introduce, on the basis of climatologies presented in part 1, the concept of a monsoon stationary wave over Australia, describe its structure and properties and discuss its interaction with mid latitude travelling waves in the context of formation of monsoon depressions and cyclones over the Australian region.

Acknowledgements

Grateful acknowledgement is made to NCEP for providing reanalysis products on which the study is based.

References

Berson, F.A. and Troupe, A.J., 1961, "On the angular momentum balance in the equatorial trough zone of the eastern hemisphere", *Tellus*, **13**, 66-78.

Davidson, N.E., McBridge, J.L., and McAvaney, B.J., 1983, "The onset of the Australian monsoon during winter MONEX; Synoptic Aspects", *Mon. Wea. Rev.*, **111**, 495-516.

Davidson, N.E., McBridge, J.L., and McAvaney, B.J., 1984, "Divergent circulations during the onset of the 1978-79 Australian monsoon", *Mon. Wea. Rev.*,**112**, 1684-1696.

Findlater, J., 1969, "Interhemispheric transport of air in the lower troposphere over the western Indian ocean", *Quart. J.R. Met. Soc.*, **95**, 400-403.

Gentilli, J., 1971, "Dynamics of the Australian troposphere. In Climates of Australia and New Zealand, ed. J. Gentilli, 53-117, World Survey of Climatology, Vol 13, Elsevier, New York.

Holland, G.J., 1984a,"On the Climatology and structure of tropical cyclones in the Australian/Southwest Pacific region. I. Data and tropical storms", *Aust. Meteor. Mag.*, **32**, 1-15.

Holland, G.J., 1984b,"On the Climatology and structure of tropical cyclones in the Australian/Southwest Pacific region. II. Hurricanes", *Aust. Meteor. Mag.*, **32**, 17-31.

Holland, G.J., 1984c,"On the Climatology and structure of tropical cyclones in the Australian/Southwest Pacific region. III. Major hurricanes", *Aust. Meteor. Mag.*, **32**, 33-46.

Holland, G.J., and Nicholl's, 1985, "A simple predictor of El Nino?" *Trop. Ocean-Atmos. News-lett.*, **30**, 8-9.

Holton, J.R., 1979, "An introduction to dynamic Meteorology (second edition), Academic Press, New York and London.

Kalnay, E., and co-workers, 1996, "The NCEP/NCAR 40-year reanalysis project", *Bull. Amer. Meteor. Soc.*, **77**, 437-471.

Love, G., 1985a, "Cross-equatorial influence of winter hemisphere cold surges", *Mon. Wea. Rev.*, **113**, 1487-1498.

Love, G., 1985b, "Cross-equatorial interactions during tropical cyclogenesis", *Mon. Wea. Rev.*, **113**, 1499-1509.

Love, G. and Garden. G., 1984, "The Australian monsoon of January 1974", *Aust. Meteor. Mag.*, **32**, 185-194.

McBride, J.L., 1983, "Satellite observations of the southern hemisphere monsoon during winter MONEX", *Tellus*, **35A**, 189-197.

McBride, J.L., 1987, "The Australian summer monsoon. In Monsoon Meterology (ed: Chang and Krishnamurti), Oxford University Press, New York, 203-231.

McBride, J.L., and Nicholls, N., 1983, "Seasonal relationships between Australian rainfall and the southern oscillation", *Mon.Wea.Rev.*, **111**, 1998-2004.

Murakami, T. and Sumi, A., 1982a,"Southern hemisphere summer monsoon circulation during the 1978-79 WMONEX. Part 1: Monthly mean wind fields", *J. Meteor. Soc. Japan*, **60**, 638-648.

Nicholls, N., 1984a,"A system for predicting the onset of the North Australian wet season", *J. Climato.*, **4**, 425-436.

Nicholls, N., 1984b, "The southern oscillation, sea-surface temperature, and interannual fluctuations in Australian tropical cyclone activity", *J. Climatol.*, **4**, 661-670.

Nicholl, N., McBride, J.L., and Ormerod, R.J., 1982, "On predicting the onset of the Australian wet season at Darwin", *Mon.Wea.Rev.*, **110**, 14-17.

Pittock, A.B., 1984, "On the reality, stability and usefulness of southern hemisphere teleconnections", *Aust.Meteor.Mag.*, **32**, 75-82.

Ramage, C.S. and Raman, C.R.V., 1972, "Meteorological Atlas of the International Indian ocean Expedition, Vol.2 (Upper Air), U.S. Govt. Printing Office, Washington, D.C., 121.

Raman, C.R.V., 1965, "Cyclonic vortices on either side of the equator and their implications," Met. Results of the I.I.O.E., 155-163.

Rao, Y.P., 1964, "Interhemispheric circulation" , *Quart. J.R.Met.Soc.*, **90**, 190-194.

Saha, K.R., 1970, " Air and water vapour transport across the equator in western Indian ocean during northen summer", *Tellus*, 1970, 681-687.

Saha, K.R., 1973, "Global distribution of double cloud bands over tropical oceans", *Quart. J. Roy. Meteor. Soc.*, **99**, 551-555.

Saha, K.R. and Saha, S., 1989, "Vertical circulations and heat and moisture budgets in the time-mean July atmosphere over India and Bay of Bengal", *Mausam*, **40**, 159-168.

Saha, S. and Saha, K.R., 1996, "Structure and properties of the summer monsoon stationary wave over southern Asia : An observational analysis", *Mausam*, **47**, 133-144.

Schemm, J., Schubert, S., Terry, J., Bloom, S., 1992, "Estimates of monthly mean soil moisture for 1979-89. NASA Tech. Memo. 10451, NASA/Goddard Space Flight Centre, Greenbelt, MD.

Spencer, R.W., 1993, "Global oceanic precipitation from the MSU during 1979-91 and comparisons to other climatologies", *J. Climate*, **6**, 1301-1326.

Sumi, A. and Murakami, T., 1981, "Large-scale aspects of the 1978-79 winter circulation over the greater MONEX region. I. Monthly and seasonal fields", *J. Meteor. Soc. Japan*, **19**, 625-645.

Tao, S. and Chen, L., 1987, "A review of recent research on the east Asian summer monsoon in China", In Monsoon Meteorology (Eds: Chang and Krishnamurti), 60-92.

Troup, A.J., 1961, "Variations in upper-troposphere flow associated with the onset of the Australian summer monsoon", *I. J. Meteor. Geophys.*, **12**, 217-230.

Van den Dool, H.M. and Saha, S., 1993, "On the seasonal re-distribution of atmospheric mass in a 10-year GCM run", *J. Climate*, **6**, 22-30.

Xie, P.P. and Arkin, P.A., 1996, "Analyses of global monthly precipitation using gauge observations, satellite estimates and numerical model predictions", *J. Climate*, **9**, 840-858.